Reviews in Mineralogy & Geochemistry
Vol. 58, pp. 527-565, 2005

Visualizing Thermotectonic and Denudation Histories Using Apatite Fission Track Thermochronology

Barry P. Kohn[1], Andrew J.W. Gleadow[1], Roderick W. Brown[2], Kerry Gallagher[3], Matevz Lorencak[1] and Wayne P. Noble[1]

[1]School of Earth Sciences
The University of Melbourne
Melbourne, Australia 3010

[2]Division of Earth Sciences, Centre for Geosciences
University of Glasgow
Glasgow G12 8QQ, Scotland

[3]Department of Earth Science and Engineering
Imperial College London, South Kensington
London SW7 2AS, England

INTRODUCTION

Thermochronology, the use of temperature-sensitive radiometric dating methods to reconstruct the time-temperature histories of rocks, has proved to be an important means of constraining a variety of geological processes. In general, different depths within the Earth's crust are characterized by different temperature regimes and processes. Within the upper crustal environment, temperature can often be used as a proxy for depth, so that reconstructed cooling histories may reveal a record of rock movement towards the surface. That portion of this process which involves temperature variations within the uppermost ~150–200 °C of crustal depth has been the basis for the application of low temperature thermochronology to a range of interdisciplinary problems in the Earth Sciences. The last fifteen or so years have sparked widespread interest in this field and this proliferation has been driven in part by advances in analytical techniques, numerical modeling, and fundamental changes of perspectives on the significance of radioisotopic ages (e.g., McDougall and Harrison 1999; Gleadow et al. 2002a; Farley 2002). One area of rapidly growing interest, which has provided unprecedented insights in this regard, has been the quantification in time and space of surface processes and shallow crustal tectonism using low temperature thermochronology, often combined with complementary techniques structural analysis, geomorphic, numerical modeling, and cosmogenic isotope studies (e.g., House et al. 1998; Ehlers and Farley 2003; Belton et al. 2004; Ehlers 2005).

One of the best established and most sensitive low temperature thermochronology methods available for reconstructing such histories in the upper ~3–5 km of the continental crust, over time scales of millions to hundreds of millions of years, is apatite fission track (AFT) thermochronology which responds to temperatures of typically <110 ± 10 °C.

As for other thermochronological methods, fission track analysis involves a geological dating technique in which the retention of radioactive decay products is sensitive to elevated temperatures. Monitoring the degree to which a particular dating system has remained closed with respect to retention of the daughter products enables the history of exposure to elevated temperatures in the geological environment to be quantified. In many cases, such thermochronometers give rise to apparent ages, which only rarely relate to the time the system

1529-6466/05/0058-0020$05.00 DOI: 10.2138/rmg.2005.58.20

was initiated. These apparent ages reflect the record of the thermal and tectonic processes which have controlled the evolution of such environments and the resulting long-term denudation patterns at the Earth's surface, rather than the original formation or depositional ages of the rocks involved. In most cases, the apparent AFT ages obtained are "mixed" ages, which reflect some integrated product of the low temperature thermal history of the crust. Only in relatively few situations do they directly date a particular discrete geological event involving rapid cooling. Therefore, the significance of regional AFT patterns is not always obvious and non-specialists have often found such seemingly intractable and unwieldy data difficult to interpret, resulting in an inability to fully visualize the implications of the results.

In this paper we show how large regional AFT data sets assembled from surface samples collected from southeastern Canada, southern and eastern Africa, and southeastern Australia, can be presented in ways that their patterns of variation can be readily understood. This allows useful geological information to be extracted in a format that can be readily combined with other large-scale data sets, e.g., digital elevation and heat flow. The terranes investigated mainly comprise crystalline rocks where conventional stratigraphic markers and cross-cutting relationships which might be useful for reconstructing their regional Phanerozoic tectonic and exhumation history are largely absent. Imaging and visualizing that part of the thermal history information contained in the AFT data therefore provides a regional framework, for quantifying the spatial coherence and variability in the timing and magnitude of cooling and crustal denudation, through a part of geological time, hitherto largely unconstrained in these terranes.

APATITE FISSION TRACK THERMOCHRONOLOGY

The general principles of AFT thermochronology, the interpretation of data and their application to geological problems have been outlined in several works (e.g., Wagner and Van den haute 1992; Brown et al. 1994b; Gallagher et al. 1998; Gleadow and Brown 2000; Gleadow et al. 2002a; Tagami and O'Sullivan 2005; Donelick et al. 2005). The process of annealing and the ability to adequately constrain the thermal response of that behavior through experiments on laboratory timescales is the key to the investigation of thermal histories by fission track studies. Briefly, AFT annealing is a thermally activated process occurring over a range of temperatures typically up to ~100–120 °C over geological time scales. With increased levels of annealing, fission tracks become progressively shorter and once a rock cools to the temperature range of relative track stability the tracks retain most of their full initial length. During annealing, tracks will shorten to lengths largely controlled by the maximum paleotemperature to which they have been exposed, so that fission track lengths can be used to provide a measure of the amount of annealing that has occurred. Each individual track is added by a radioactive decay event at a different time, and thus experiences a different fraction of the thermal history. Hence, the lengths of individual tracks are related to the paleotemperatures experienced by samples over different time intervals. Because of the numerous possible time-temperature paths experienced by a particular sample, it is clear that an AFT age alone can be interpreted in a number of ways (e.g., Gleadow and Brown 2000). Considering the AFT age and length data together however, reflect a combination of the time over which tracks have been retained as well as the thermal history of the host rock over that period. Integration of the age and track length parameters can therefore place rigorous constraints on the history of cooling through the fission track annealing zone, e.g., fast or slow cooling or more complex types (Gleadow et al. 1986). Since apatite is the mineral for which annealing systematics are best understood and because it typically contains uranium in the 1–100 ppm range and is a common accessory mineral in many rock types, AFT thermochronology is almost universally applicable to large areas of the Earth's continental crust.

THERMAL HISTORY MODELING

The kinetics of fission track annealing can be studied at higher temperatures for times ranging from hours to years in the laboratory using controlled heating experiments on fresh, neutron-induced ^{235}U fission tracks. These are essentially identical to the natural ^{238}U tracks used in geological dating. Such laboratory annealing studies have given rise to quantitative models of fission track annealing in apatite (e.g., Laslett et al. 1987; Corrigan 1991; Crowley et al. 1991; Carlson et al. 1999; Donelick et al. 1999). These annealing models can in turn be used to calculate the AFT age and track length distribution with the least amount of variance that would result from any given thermal history on a geological time scale (e.g., Green et al. 1989; Ketcham et al. 1999). In order to extract the most plausible thermal histories from the observed AFT data inversion modeling procedures are used. For modeling purposes various mathematical approaches for sampling time-temperature space have been described (e.g., Corrigan, 1991; Lutz and Omar 1991; Gallagher 1995; Willett 1997) and several software applications have been developed to automate the procedure (e.g., Crowley 1993; Gallagher 1995; Issler 1996; Ketcham et al. 2000; Ketcham 2005). Where possible any additional geological information and temperature information can also be incorporated into models to provide more relevant time-temperature constraints.

For the studies described here we have adopted the approach of Gallagher (1995) which uses the algorithm reported by Laslett et al. (1987) to simulate the time-temperature dependence of fission track annealing in apatite as determined from a detailed set of laboratory experiments. The modeling procedure uses a stochastic search method for exploring a wide range of possible thermal histories with statistical testing of the predicted fission track age and length parameters against the observed values. Since the possible solutions that satisfactorily match the observed data are not necessarily unique, a guided search by means of a genetic algorithm (Gallagher and Sambridge 1994) is used to sort through a large search (typically thousands) of potential thermal history histories. The maximum likelihood or probability of each time-temperature path is assessed, providing rapid convergence towards an optimal fit of the observed data. The model thermal history procedure can be refined to be locally optimal and it is then possible to also define the confidence limits around a path (Fig. 1). The application of such inverse approaches to AFT modeling has generally focused on the thermal history inference for individual samples. Increasingly however, there is a necessity to consider the results of thermal history modeling in a more regional context, using larger sample arrays.

REGIONAL APATITE FISSION TRACK DATA ARRAYS

An important consequence of fission track annealing is that fission track ages in general, gradually decrease from some observed value at the Earth's surface to an apparent value of zero at the depth where no fission tracks are retained. The depth to the base of this fission track annealing zone will depend on the geothermal gradient and the annealing properties of the particular apatites being studied (see below). The shape of an AFT age profile, such as may be obtained in an area of high relief or from a deep borehole, will reflect the thermal history of the rocks as they cooled through the annealing zone. Such profiles will vary for different thermal history styles (Gleadow and Brown 2000).

The importance of such vertical arrays of samples is that they contain more information than that which can be obtained from any individual sample alone (Gallagher et al. 2005). Because of the fixed geometric relationship that the samples have to each other, in most cases they are constrained to have followed essentially parallel temperature-time histories. Such a sampling approach does not lend itself so readily to large continental regions where there

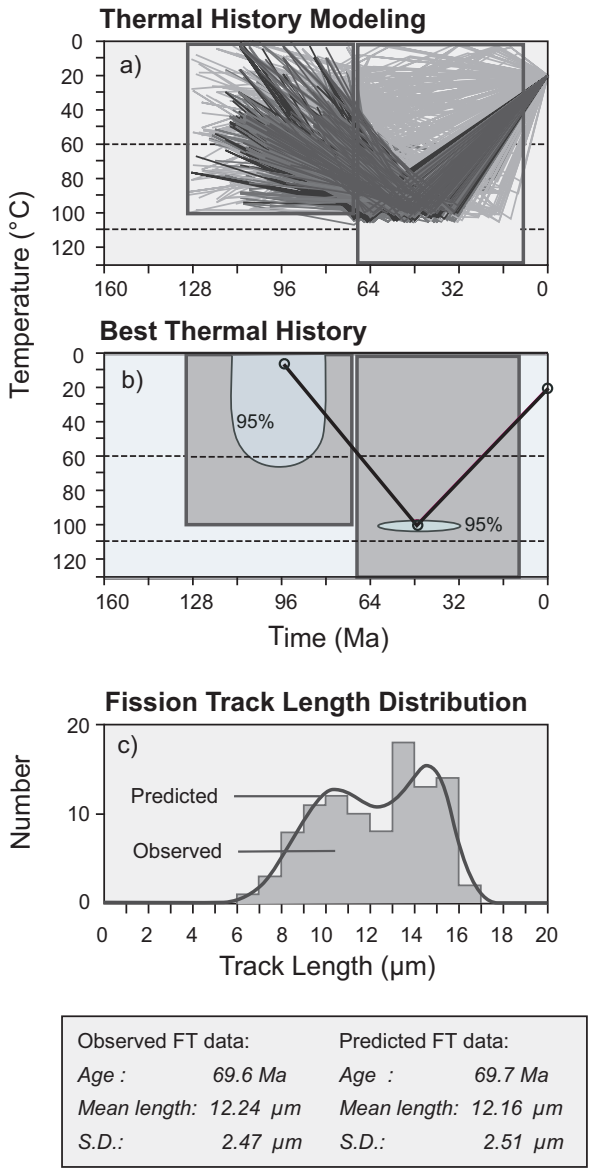

Observed FT data:		Predicted FT data:	
Age :	*69.6 Ma*	*Age :*	*69.7 Ma*
Mean length:	*12.24 μm*	*Mean length:*	*12.16 μm*
S.D.:	*2.47 μm*	*S.D.:*	*2.51 μm*

Figure 1. Time-temperature inversion modeling of apatite fission track data. Panel (a) searching time-temperature space, here defined by two boxes, using a Monte Carlo approach for a best-fit two stage thermal history from some 10,000 randomly generated paths. The dark grey paths are those that satisfactorily match the measured apatite fission track data (age, mean confined track length and confined track length distribution). Panel (b) shows the optimal-fit thermal history path determined by employing a guided search by means of a genetic algorithm (Gallagher and Sambridge 1994) and assessment of the maximum likelihood of each path, with the 95% confidence limits around key points on the path. Panel (c) histogram showing the observed track-length distribution compared with that predicted from the optimal-fit thermal history path. The lowermost panel shows a numerical comparison of the input observed fission track data and the predicted estimates of fission-track age, mean track length and standard deviation of the track length distribution arising from the best-fit thermal history path shown in (b) above.

is relatively little relief (or minimal deep borehole data) and for which the assumption of a common cooling history is clearly not appropriate. An alternative approach, suitable for the rapid interpretation of large regional data sets of outcrop samples, is to sequentially model the thermal histories for all samples in an array using a common search strategy. In this case the thermal histories are not constrained by neighboring samples, as they would be in a vertical profile but are free to vary independently from each other. However, using common search parameters (e.g., fission track age, mean track length and track length distribution) and model time-temperature space encourages consistency between the thermal histories for different samples, and will reveal similarities if such information is implicit in the data. The results of this modeling approach can then be interpolated spatially to link the paleotemperatures for individual samples over a consistent set of time steps. Note that this approach does not quantitatively link the thermal histories of nearby samples as in the partition modeling approach described by Gallagher et al. (2005). However, this does represent an end member case in that each sample is effectively allocated a separate partition.

QUANTIFYING LONG-TERM DENUDATION

AFT thermal history information may be related to thermal relaxation following increased heat-flow (for example related to rifting), to localized magmatism, hot fluid flow or to denudation at the land surface. Thermal modeling studies have thus far indicated however, that the direct thermal effects of rifting are unlikely to be significant within the shallow crust environment (≤~10 km) of the onshore regions of margins (e.g., Buck et al. 1988, Gallagher et al. 1994b, Brown et al. 1994a). The movement of hydrothermal fluids in former cover successions or structural pathways in crystalline basement may influence the AFT pattern in some cases but generally this is viewed as a more localized effect (e.g., Steckler et al. 1993; Duddy et al. 1994; Gleadow and Brown 2000; Gleadow et al. 2002b). Magmatism, also, is mostly restricted locally rather than regionally in the areas reported here. Hence, most cooling in the near-surface environment is dominated by tectonic and erosional denudation. Therefore, a principal assumption in our studies is that it is usually the amount of denudation and the pattern of tectonic offsets that causes the variation in apparent AFT ages at the land surface. Consequently, AFT data can be used to reconstruct regional denudation patterns (e.g., Gallagher and Brown 1999a,b).

Assumptions and uncertainties

Paleotemperatures, heat flow and thermal conductivities. Estimates of long-term denudation are made by converting temperature histories (typically estimated to have an uncertainty of ~10 °C for the paleotemperature at any given point) to an equivalent depth history by making assumptions regarding past heat flow and surface temperatures, as well as the thermal conductivity of the material eroded (Gallagher and Brown 1999a; Gleadow and Brown 2000; Brown et al. 2002). Where vertical profiles are available paleogeothermal gradients may be estimated for time modeled maximum paleotemperatures prior to the onset of cooling (e.g., Brown et al. 2002; Gallagher et al. 2005). For most situations however, where only surface samples are available, it is difficult to constrain past paleogeothermal gradients and the thermal conductivity of the missing section explicitly, unless some form of joint modeling can be used (Gallagher et al. 2005). Region specific geothermal gradients may be extracted from the global heat flow data set of Pollack et al. (1993) and these data suggest that the range of continental gradients in Precambrian and Paleozoic crystalline terranes is relatively restricted (with a mean between ~20–30 °C·km^{-1}) and that large anomalies are usually localized. Further, errors arising from anomalous transient thermal gradients could be significant, but even in extreme cases are unlikely to be greater than a factor of ~2 (Gleadow and Brown 2000). In sedimentary basins where thermal conductivities are generally lower

however, geothermal gradients may be more variable and it may also be possible to estimate past gradients in conjunction with vitrinite reflectance studies (e.g., Bray et al. 1992).

Results using a constant as opposed to a spatially variable present day heat flow show that in general, the timing of enhanced episodes of denudation do not differ markedly, although the magnitude may vary (Kohn et al. 2002a; Gunnell et al. 2003; see also Fig. 2). This assumption along with others (e.g., assumed constant thermal conductivity of the eroded section, surface temperature and paleogeothermal gradient) clearly limit the accuracy of long-term denudation rate estimates, which are considered here only as a first-order approximation (see also Brown and Summerfield 1997).

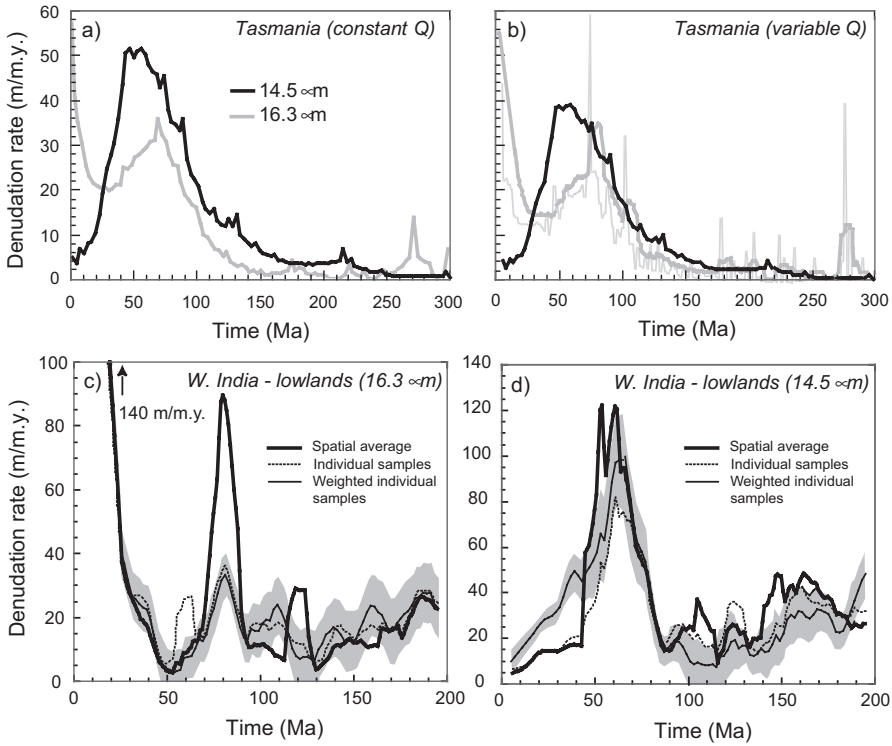

Figure 2. Long-term smoothed (spatially averaged) denudation chronology plots for Tasmania (a and b, modified after Kohn et al. 2002) and the lowlands of western peninsular India (c and d, modified after Gunnell et al. 2003). The spatial average (bold curve in all plots and light curve in plots a and b) is based on interpolating the results over each study area; the individual sample curve (very light curve in plot b and dashed curve, plots c and d) is the unweighted mean of the denudation chronology at individual locations; the weighted sample curve (plots c and d, thin solid line) is the mean denudation at individual locations, weighted by the uncertainty in the inferred thermal history for each location. The shaded area (plots c and d) is the standard error on the weighted mean estimate and is considered to indicate the magnitude of uncertainty inherent in the modeling procedure. Plots (a) and (b) also compare the effects of spatially and temporally constant heat flow (60 $mW \cdot m^{-2}$) and spatially variable but temporally constant (i.e., present day pattern) heat flow (Q). Use of different heat flow parameters leads to differences in magnitude of denudation rates but with no marked change in the timing of periods of accelerated denudation. The effect on denudation chronology of using initial track lengths of 16.3 μm (light line) and 14.5 μm (bold line) are also shown (plots a and b, and plot c versus d). The utilization of initial track lengths of 16.3 μm for thermal history modeling leads to the inference of major cooling and hence dramatically increased denudation rates during the mid to late Tertiary (see text for further discussion).

If paleogeothermal gradients were elevated at the time of a particular period of denudation compared to those of the present day then the actual magnitude of denudation would be lower (as would the calculated long-term denudation rate). For the terranes reported here we have not considered variations of heat flow with time, as we have no constraints on how this may have occurred, except perhaps at some of the rifted continental margins. As mentioned previously however, the influence of rift-related heat flow variations tend to be relatively minor in the rift flanks where some of the onshore samples studied were collected (e.g., southeastern Australia, southern and eastern Africa) and is expected to be even less significant elsewhere.

Compositional variations. Annealing properties of fission tracks in apatite vary with duration of heating, chemical composition (Gleadow and Duddy 1981; Green et al. 1985; Barbarand et al. 2003) and mineralogical properties (Carlson et al. 1999). The total annealing temperature for chlorine-rich apatites for example, occur at higher temperatures ~110–150 °C compared to that in the more common fluorine-rich apatites ~90–100 °C (e.g., Green et al. 1985; Burtner et al. 1994). Although chlorine substitution probably exerts the most important effect, the possible influence of other trace elements (including rare earths) has also been reported (Barbarand et al. 2003).

In the regions studied the rocks sampled are of limited compositional range (mostly granites and granodiorites) and the apatites they contain are mainly fluorine-rich apatite. This has been confirmed by electron microprobe analyses of a representative sampling of grains (mostly <0.2 wt% chlorine) and the qualitative consideration of apatite solubility in that the track etching rate and etch pit size are known to correlate with chlorine content (Donelick 1993; Barbarand et al. 2003). Fast etching grains, likely to be of more extreme composition and hence displaying different annealing properties (Burtner et al. 1994; Carlson et al. 1999), were generally avoided for the AFT analyses presented here. However, in the case study from southern Canada some higher chlorine content apatites were observed and their effect on the measured AFT parameters can be clearly seen (Plate I). For other areas studied we consider that the annealing properties of the apatites analyzed represent a coherent set in terms of their annealing properties and do not depart to a significant degree from the Durango apatite composition of ~0.4 wt% chlorine upon which the Laslett et al. (1987) annealing model is based. It is probable that the average chlorine content will be lower than this Durango apatite value suggesting that paleotemperatures reconstructed on this basis may be too high in some cases, possibly by as much as ~10–15 °C, but are unlikely to be too low.

Modeling strategies. The annealing model of Laslett et al. (1987), the model adopted here to obtain long-term denudation rates, is formulated in terms of the current measured track length normalized to an initial track length. This is referred to as the reduced track length and is defined as $r = l/l_0$, where l and l_0 are the annealed and "unannealed" track lengths, respectively. In applications of the original model formulation, using an initial track length of 16.3 μm, the lack of low temperature annealing typically leads to the inference of major cooling in the geologically recent past (Kohn et al. 2002; Gunnell et al. 2003). This can be alleviated partly by considering what the initial track length parameter represents in these annealing models. Mean spontaneous track lengths from rapidly cooled geological samples rarely exceed ~14.5 to 15 μm while the mean lengths from "unannealed" induced tracks are typically 16.3 ± 0.9 μm (Gleadow et al. 1986; Green 1988). Donelick et al. (1990) showed that the initial length of induced tracks is not constant over very short times and that room temperature annealing occurs in a matter of days. It is clear then, that the generally assumed initial track length is itself a variable, implying that 16.3 μm may not be the relevant unannealed track length over geological timescales. Hence, for geological timescales, spontaneous tracks may effectively be ~10% shorter than that observed on laboratory timescales for induced tracks (Gleadow et al. 1986; Laslett and Galbraith 1996, Ketcham et al. 1999). As a consequence, the Laslett et

al. (1987) model, based on the laboratory determined initial length does not appear to predict sufficient annealing at temperatures lower than ~50–60 °C.

As a model calibrated for reduced track lengths depends strongly on the assumed initial track length we have compared the effect of two initial track length values, i.e., 16.3 and 14.5 μm on the modeled thermal histories of two different terranes (Fig. 2). The former value is that inferred for induced tracks, while the latter is consistent with the maximum value typically observed from spontaneous tracks in surface geological samples, assumed to have undergone little post-formation thermal disturbance. In considering regional denudation in this work we have used the latter value. It is acknowledged that this is a departure from an initial length of 16.3 μm upon which the Laslett et al. (1987) model is based and that further refinement and treatment of initial length estimates to account for the observed amount of annealing is required. Strategic approaches to tackle this problem have been outlined by Gunnell et al. (2003).

Data for each sample from southern Africa, eastern Africa and southeastern Australia were modeled to produce optimal data fitting thermal histories. As we are dealing entirely with surface or very shallow samples, we used a scheme to encourage cooling in the thermal history by starting models at high temperature and fixing the present day surface temperature appropriate for the relevant study area. The points in-between can show cooling followed by reheating (e.g., a saw tooth pattern). Rapid temperature variations are damped out as these are poorly constrained by the original data and cannot resolve well the amount of cooling below the subsequent reheating event. Further, any temperature points less than the maximum of a more recent reheating event are moved so that the cooling only proceeds to 5 °C below the subsequent reheating maximum, but such that the rate of the previous cooling event is maintained. If there is more than one point in the cooling episode it is removed, as it makes no difference to the data fit relative to the damped thermal history. This approach implicitly minimizes variations in the thermal history that are unconstrained by the observed data, e.g., multiple episodes of heating and cooling.

Regional-scale imaging

A flow chart showing the various possible inputs and outputs which can be used in applying fission track modeling to the imaging of thermal history, denudation and paleotopography estimates is shown in Figure 3. By combining denudation information with digital elevation data, it is possible to model the evolution of paleotopography. The paleotopography is estimated by "backstacking" the amount of section removed by denudation in a given time period onto the current surface elevation at that location and allowing the back-stacked column to regain isostatic equilibrium (Brown 1991). This is achieved by using a regional flexural isostasy using a thin plate model with an effective elastic thickness of 25 km (Gallagher and Brown 1999b). Estimating the paleotopography between data points requires adding the inferred overburden to a smoothed topographic surface and applying an isostatic correction. Such reconstructed "paleoelevation" estimates need to be interpreted with some caution as they only reflect the passive response to denudation unloading and do not take into account any possible transient episodes of tectonic uplift, subsidence relative to the present land surface or correction for local deformation and/or faulting.

As a consequence of propagating multiple sources of uncertainty from earlier stages, the farther removed the information sought is from the primary fission track data (Fig. 3), the greater will be the cumulative uncertainties associated with them. These include the analytical uncertainties inherent in the data and the annealing model adopted, as well as uncertainties in assumptions regarding paleoheat flow, thermal conductivity, surface temperatures, thermal equilibrium in the crust when converting temperature to depth/denudation and isostatic mechanisms when calculating paleoelevation. Subject to an awareness of these various uncertainties a set of images can be constructed for any particular time-slice for which the

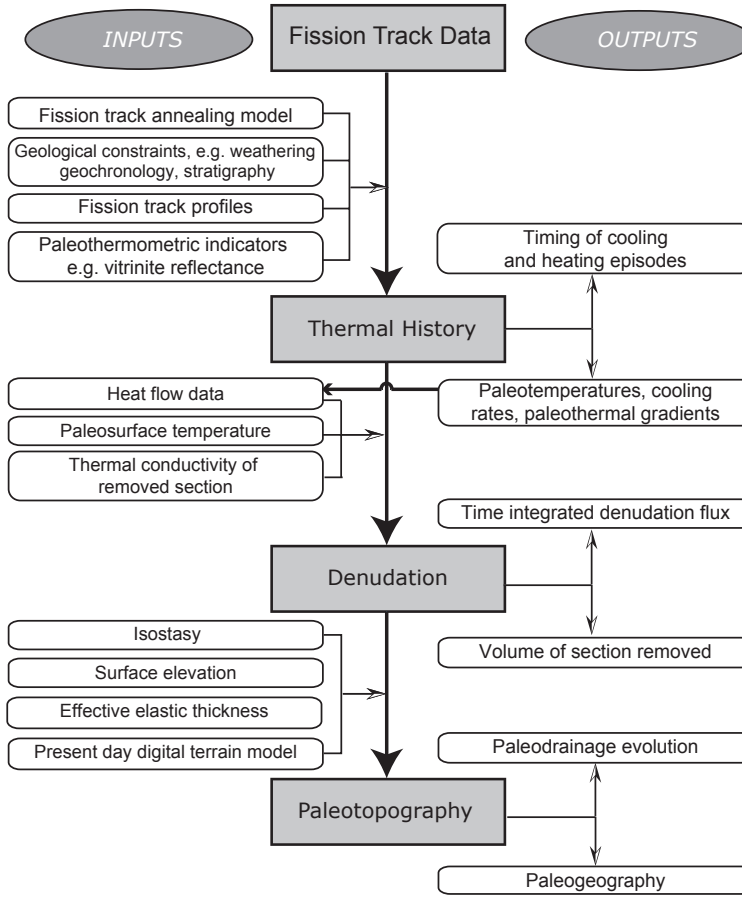

Figure 3. Flow chart showing the sequence of steps and possible inputs which can be used to determine geologically useful outputs from regional apatite fission track data. It is also possible to display as images the regional thermal history, magnitude of denudation and paleotopography for different time slices (see text and Fig. 4 and Plates II-IV). Sources of error are cumulative so that uncertainties increase with each step away from the original apatite fission track data (see text for further discussion on sources of uncertainty) (modified after Kohn et al. 2002; Gleadow et al. 2002a).

modeled temperature remains within the AFT annealing window (Fig. 4). The resulting individual time-temperature solutions can then be "stacked" and visualized as a sequence of regional time-slice images which, when combined into a computer animation depict how temperature, denudation and elevation of present day surface rocks have varied during their passage through the upper crust (e.g., Gleadow et al. 1996; Gallagher and Brown 1999a,b; Kohn et al. 2002). Although such images are extremely useful for visualizing the evolving thermal history for large regional data sets, they can only be considered as broad estimations because the process of bulk modeling and interpolation removes some of the detail that can be obtained during an assessment of the thermal histories of individual samples.

To produce the images, interpolation of the modeled data was carried out with Generic Mapping Tools software (Wessel and Smith 1991) using an adjustable tension, continuous curvature surface gridding algorithm (Smith and Wessel 1990). Interpolation was performed

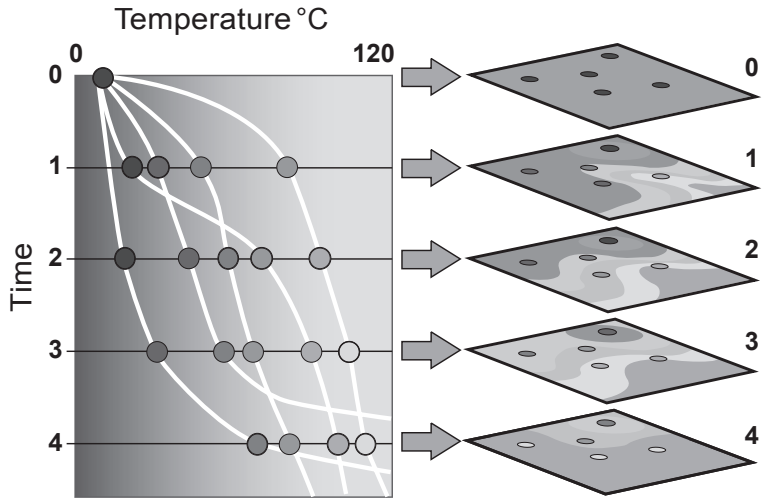

Figure 4. Derivation of paleotemperature images. Following the sequential thermal history modeling of samples within a regional subset, a series of time-temperature curves (white lines, left panel) are derived. Then for different nominal time slices (1-4) paleotemperatures for different samples (filled circles) can be spatially interpolated on a regional map and compiled as a series of time-slice image stacks. Such stacks can then be visualized as a time sequence (and also as a digital movie) showing how temperature of present day surface rocks has varied through time. Such stacks can also be extended to image denudation and paleotopography (see Fig. 3 and text).

across regional data sets for any particular parameter in a time-slice, e.g., paleotopography, but masked to exclude regions where no data were available within a specifically defined distance.

Denudation chronologies

Thermal and denudation histories inferred from AFT data can also be summarized and made more accessible by presenting the results in terms of their spatially integrated denudation rate history. Whereas results from previously published work tend to emphasize the detailed aspects of cooling histories of individual samples, the more regional representation quantifies the average denudation rate as a function of time from multiple samples. This approach takes the denudation chronology inferred for each sample and uses a nearest neighbor interpolation method (Sambridge et al. 1995) to produce a spatial grid of denudation at each time scale. This grid is then integrated spatially at successive time-slices to derive a regional denudation chronology. This scheme satisfies the observed data exactly, and uses weighting based on the spatial distribution of the data points to perform interpolation. This method does not rely on splines (e.g., Mitas and Mitasova 1995), and so does not suffer from the common problem of unconstrained features in the interpolated field. For the case histories presented from Tasmania, southeastern Australia and the lowlands seaward of the Western Ghats escarpment, India (Fig. 2) we interpolated the model results (e.g., paleotemperature, denudation) onto a grid, with a spacing of approximately 10 km. We generated these spatial grids for the results at 2 Ma intervals back to 300 Ma.

One easy way of representing the results is to integrate the spatial denudation information for each time interval, to produce the locally averaged denudation rate as a function of time, or denudation chronology (e.g., Gallagher and Brown 1999a,b). In Figure 2 we represent the denudation chronologies both as the raw integrated estimates and five point smoothing (i.e., over 10 Ma) on these estimates. The smoothing (the spatial average) is used because,

although discrete short cooling episodes (and by inference denudation) can occur, there is some uncertainty on the timing, which is not incorporated into the interpolation/integration process. Thus, the amplitude of such rapid cooling/denudation may not be as high as implied by the raw estimates, or as rapid (Fig. 2b-d). The smoothed curves serve to highlight this implicit uncertainty.

Clearly, as we are using interpolation, there will be some uncertainty and possible artifacts in the denudation chronology as a consequence of the interpolation procedure (e.g., Brown et al. 2001). There are various ways to assess this procedure, for example cross-validation and bootstrapping (Efron and Tibshirani 1993) or using kriging as the interpolation scheme (Isaaks and Srivastava 1989). We illustrate one very simple approach for western peninsular India (Fig. 2c,d) where we compare the denudation chronology determined from spatial interpolation and integration, with the denudation chronology averaged over the individual samples, with no interpolation. We also show a weighted average denudation curve, where the weighting is equivalent to the uncertainty on the individual thermal histories for each sample. Our motivation for this is that features, which consistently appear in the different estimates of the denudation chronology, are not likely to be artifacts of the interpolation process.

In making such first-order long-term denudation reconstructions some of the assumptions as detailed above should be borne in mind, as all of them will introduce uncertainties. Such assumptions clearly limit the accuracy of the denudation magnitude and rates, although the timing of enhanced denudation phases appears to be robust to physically reasonable variations in these parameters.

REGIONAL APATITE FISSION TRACK DATA ARRAYS

Southern Canadian Shield – record of a foreland basin across a craton

Geological overview. The Canadian Shield in Ontario consists mainly of the Archaean Superior Province and Proterozoic Southern Province (Fig. 5). To the southeast, the craton is bordered by the 1–1.3 Ga Grenville Province. The geological development of the shield has been discussed by Hoffman (1988), Thurston et al. (1991) and Lucas and St-Onge (1998).

Southeastern Ontario was subjected to rifting during the Late Proterozoic, resulting in the formation of graben structures such as the Ottawa-Bonnechère and Lake Timiskaming grabens (e.g., Kumarapelli 1985 and Fig. 5). Transition to a compressional regime followed during the Paleozoic, characterized by accretion of the Appalachian Orogen to the southeast. Three principal orogenic phases are usually distinguished: the Late Ordovician Taconic orogeny, the Late Devonian Acadian orogeny and the Carboniferous-Permian Alleghenian orogeny. On the shield itself, a number of structural arches developed during the Paleozoic. These represent areas of repeated cratonic uplift and criss-cross the craton in dominant northeast and northwest trends; basement arch movements may have been triggered and controlled by plate motions and related orogenic activity at or beyond the margins of the craton (e.g., Sanford et al. 1985 and Fig. 5). Paleozoic intracratonic basins; Moose River Basin to the north, Williston Basin to the west and Michigan Basin to the south are located in depressions between the arches and surround the craton (Fig. 5), their formation is however poorly understood. While today the basins are deeply eroded, outliers of Mid-Ordovician sediments in Eastern Ontario suggest a greater paleo-extent of sediments and burial of parts of the craton during the Paleozoic.

Present day heat flow of both the Superior and Grenville Provinces is similar, with average values of 42 ± 10 $mW \cdot m^{-2}$ and 41±11 $mW \cdot m^{-2}$, respectively (Guillou-Frottier et al. 1995; Mareschal et al. 2000). Major spatial and temporal variations are not observed, and the study area can be considered as a single heat flow province (Guillou-Frottier et al. 1995).

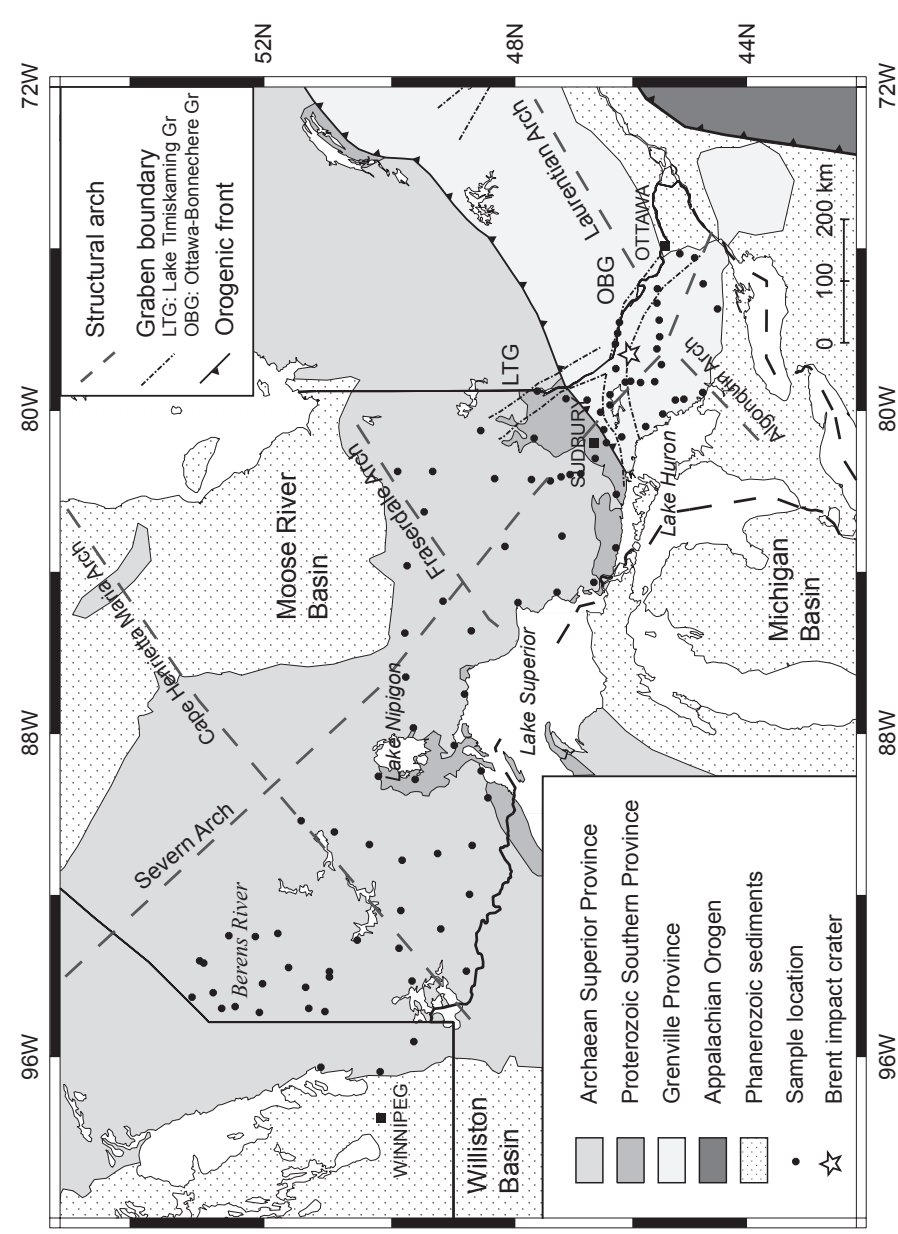

Figure 5. Geological map of the southeastern Canadian shield and adjacent sedimentary basins, showing major tectonic units, structures and apatite fission track sample locations.

Sampling for this regional reconnaissance study focused on the exposed part of the Canadian Shield and the Grenville Province across Ontario, following major roads and extending from easternmost Manitoba to Ottawa (Fig. 5). Fernando Corfu also provided a series of apatite samples from the Berens River province in western Ontario (Fig. 5), from which U-Pb apatite studies had been previously carried out (Corfu and Stone 1998). Regional surface sampling is complemented by 19 samples from a 3440 m deep drillhole in the Sudbury Igneous Complex (Lorencak et al. 2004).

Fission track results. AFT analysis was carried out on 93 samples and the regional distribution of central fission track ages and mean track lengths for apatites are shown in Plate Ia and b respectively. Apparent AFT ages range from ~600–140 Ma and all are considerably younger than the age of crystallization or metamorphism of their host rocks. The oldest ages are found north of Lake Superior, mainly ~500 Ma and these decrease to ~350–400 Ma towards western Ontario and the Berens River area. A similar decrease in age is observed towards the east; northeast of Lake Superior and north of Lake Huron, where most apparent AFT ages fall around ~350–400 Ma. This pattern changes progressively towards southeastern Ontario. There, a relatively rapid decrease in apparent AFT ages across the southern Superior and Grenville Provinces, with the youngest ages of ~140−160 Ma are observed in the vicinity of the present-day sedimentary cover of the shield.

Apatite chemistry was determined by electron microprobe analysis on representative samples and also estimated qualitatively from etch pit diameters in other samples. Most samples are fluorapatite with only a trace of chlorine (up to 0.03 wt%). The exception is from a few samples surrounding Lake Nipigon in central Ontario (Plate I) from the Nipigon diabase, where apatite chlorine content of up to 1.0 wt% was measured.

Mean horizontal confined track lengths (HCTL) range from 13.8–10.5 μm. Most fall into the range of ~11.5–12.2 μm across much of central and western Ontario. One noticeable exception is the few samples from the relatively chlorine-rich apatites of the Nipigon diabase. A second group of relatively long mean HCTL is noticeable in the northeast of the study area along the Fraserdale Arch. Similarly to the apparent AFT ages however, the most prominent change in the mean HCTL pattern is observed towards the southeast, where the increase in mean track lengths mirrors the decrease of AFT ages.

Thermotectonic history. Thermal histories of areas in the study region featuring the oldest apparent AFT ages, immediately north of Lake Superior and between the Cape Henrietta Maria and Fraserdale Arches (Plate Ia) are difficult to constrain due to the lack of independent geological observations. Time-temperature models suggest a mid-Paleozoic heating-cooling event, during which some of the tracks were partially annealed, followed by cooling during the Late Paleozoic. Further north and west, where the apparent AFT ages decrease to ~350−400 Ma, cooling was probably significantly slower and extended into the Mesozoic.

By contrast, in the eastern half of Ontario geological information provides more independent controls for the modeled thermal histories. In the Lake Timiskaming Graben in eastern Ontario, Mid-Ordovician clastic sediments directly overlie the crystalline basement, implying that the present day outcrops of the shield must have been close to the surface in early Paleozoic time. Similarly, undeformed sediments of the same age range fill the ~450 Ma Brent impact crater in southeastern Ontario (Fig. 5). Such constraints can be included into time-temperature models, such as applied to the Sudbury profile (Figs. 5 and 6) (Lorencak et al. 2004).

In the northeastern corner of the study area, along the Fraserdale Arch, a few samples display greater mean track lengths, but with apparent AFT ages in a range similar to the surrounding region (Plate Ia). Models suggest peak paleotemperatures of near-total annealing during Silurian-Early Devonian time, followed by Carboniferous cooling.

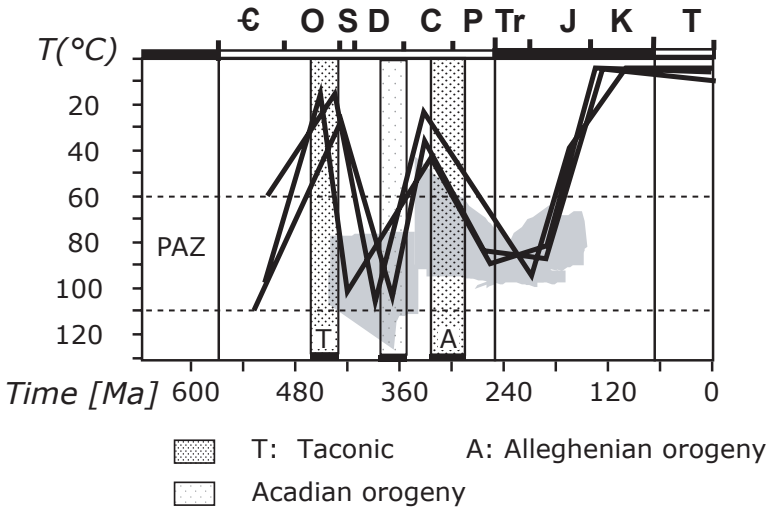

Figure 6. Modeled *t-T* paths from a near-surface sample in the Sudbury drill hole. Three equally possible best-fit paths are shown, all overlapping within 95% confidence intervals (represented by shaded areas) and each determined from 1500 model iterations, following the procedure of Gallagher (1995). Timing of the three main stages of the Appalachian orogeny are shown for comparison. PAZ = apatite partial annealing zone (modified after Lorencak et al. 2004).

Progressing towards the south however, observed track length distributions change. While most of the region north of Lake Huron retains the record of a Paleozoic thermal event, progressive younger thermal overprinting is observed. This is documented by the decrease of apparent AFT ages towards the southeast (Plate Ia), until complete resetting is attained in the Grenville Province, as indicated by Mesozoic AFT ages and a significant increase in mean HCTL (Plate Ib).

Geological implications of the thermal event, reflected in the AFT data from southeast Ontario, can be found in the Michigan Basin immediately south of the study area. The basin contains ~4.5 km of Paleozoic sediments ranging in age from Late Cambrian to Pennsylvanian (Fischer et al. 1988). Only ~200 m of Pennsylvanian age section is preserved and this is directly overlain by local, thin Jurassic red beds. Nevertheless, evidence from organic indicators suggests a greater overburden existed in late Paleozoic time. Vitrinite reflectance values (R_0) of the surface rocks are >0.55 and the Thermal Alteration Index values (TAI) >2.5 (Cercone 1984; Cercone and Pollack 1991). In the central and northern part of the basin, the oil window (R_0 >0.65 or TAI >0.65) extends up to 500 m below the present surface (Cercone 1984). Hydrocarbons from Silurian and Devonian strata similarly require either higher paleotemperatures for their in-situ generation or alternatively their upward migration by up to 2 km, in some cases through impermeable salt beds (Nunn et al. 1984). On the shield itself, AFT studies carried out on a vertical profile from a 3440 m deep drill hole in Sudbury suggest Permo-Triassic heating followed by Late Triassic-Early Jurassic cooling (Lorencak et al. 2004). This cycle has also been previously observed using AFT analysis in other parts of the shield and the Michigan Basin (Crowley 1991).

The present data set also records Permo-Triassic heating followed by Late Triassic-Early Jurassic cooling; this is in accord with the geological observations described above and with the timing suggested by previous work. The most likely cause for a regionally coherent AFT

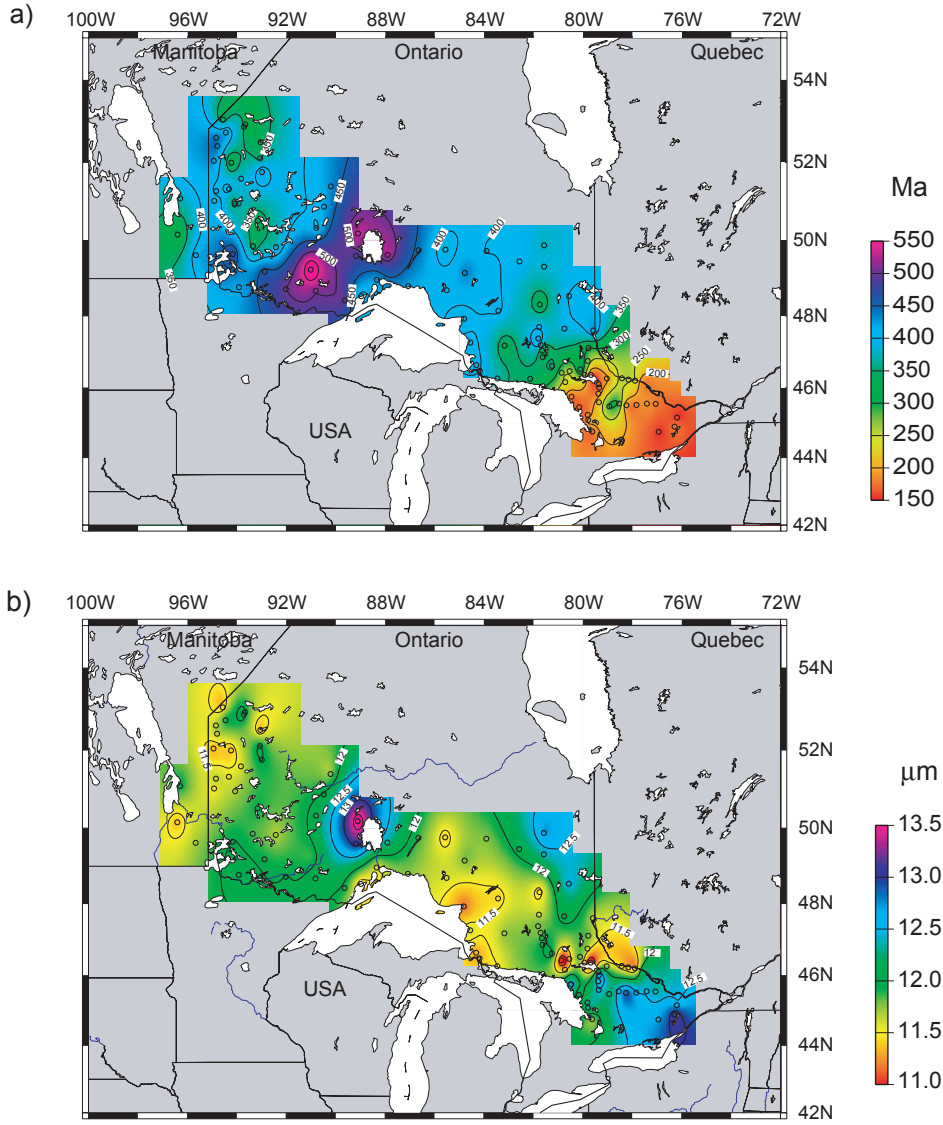

Plate I. Interpolated contour plots of apatite fission track results from surface samples across the southeastern Canadian shield showing: (a) the distribution of apparent apatite fission track "central" ages, and (b) the mean horizontal confined fission track lengths (HCTL) in microns (modified after Lorencak 2003). See also caption for Plate III for information on contouring procedure.

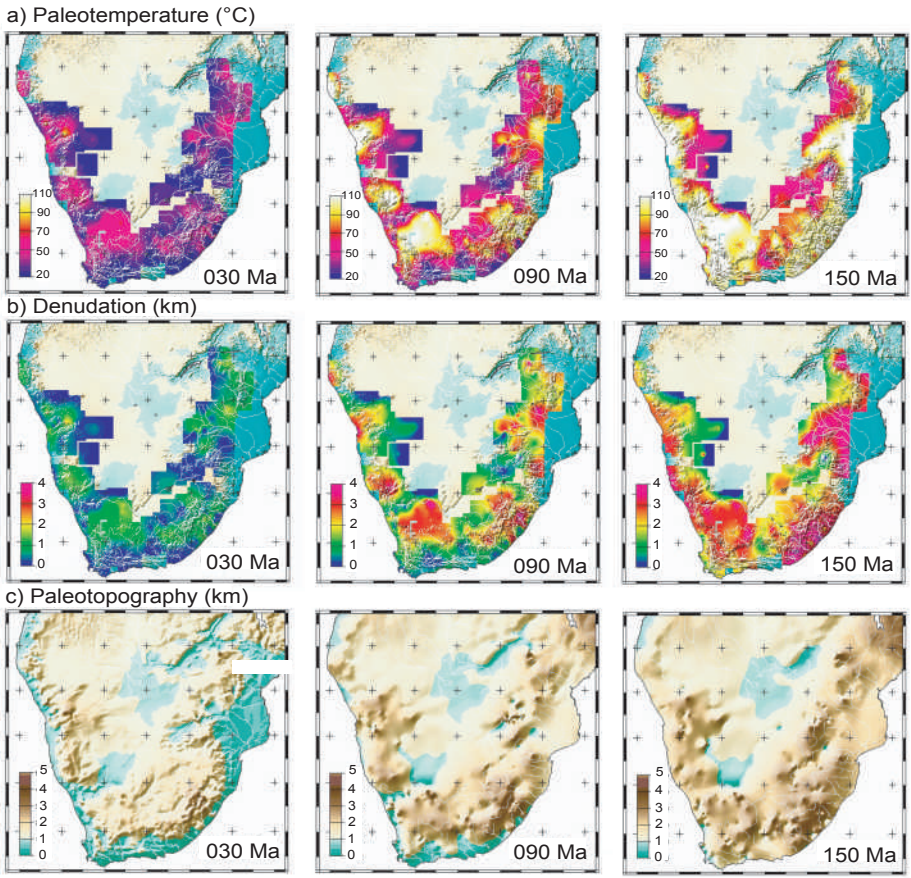

Plate II. Images showing the reconstructed (a) paleotemperatures experienced by rocks now at the surface, (b) the amount of denudation, and (c) an estimated reconstruction of paleotopography for southern Africa for four three separate time-slices; Late Jurassic (150 Ma), mid Cretaceous (90 Ma) and Oligocene (30 Ma). Paleotopography is based on "back-stacking" the present topography using the digital elevation data with the estimated amount of denudation and adjusting for an effective elastic thickness (Te) of 25 km (see Fig. 3 and Gallagher and Brown 1999a; Gleadow and Brown 2000). See also caption for Plate III for information on contouring procedure.

Plate III. (*caption continued from facing page)*
Data Center, Boulder. Colorado, USA) Global Heat Flow data set and is compiled from the work by Pollack et al. (1993). White circles indicate measurement localities, (e) contour images of post Early Jurassic temperature evolution in five time slices (180 Ma, 120 Ma, 90 Ma, 60 Ma and 30 Ma) of apatite fission track samples from eastern Africa and (f) contour images of the amount of cumulative post Early Jurassic denudation occurring across eastern Africa. The slices were generated by contouring the product of paleotemperature estimates (e) geothermal gradient (based on estimates displayed in d). Contouring of data shown in (a) to (f) was accomplished using GMT-3 (Generic Mapping Tools version 3.0 (Wessel and Smith 1991) using the commands of Surface and Blockmean with a contour interval of 30″ (background topography as for Fig. 7). Areas of no data control have been masked out using the command psmask (GMT-3.0) using a confidence interval of 1°. Note that only samples with age, track length and standard deviation information were used to generate the images shown in (e) and (f), therefore not all samples show in (a) were used for image compilation.

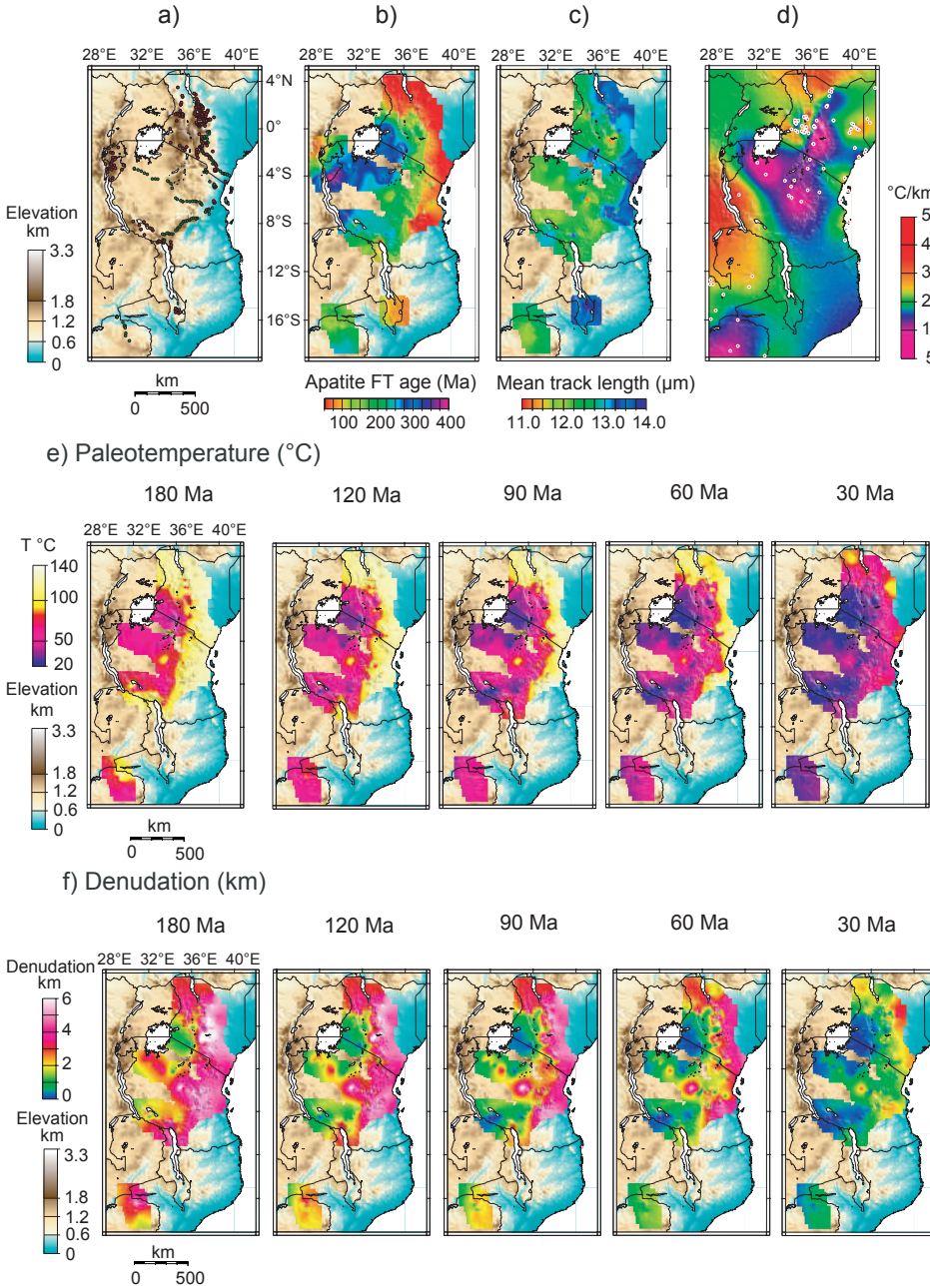

Plate III. Contour images of the AFT data collected in eastern Africa (generated using GMT-3, Wessel and Smith 1991); (a) sample locality map – green dots for samples collected in studies reported by Noble et al. (1997) and Noble (1997), red dots for samples collected in previous studies to that of Noble and co-workers (see text for further details), (b) contour image of apatite fission track ages, (c) contour image of apatite fission track mean lengths, (d) contoured present geothermal gradient values across eastern Africa used to derive the denudation estimates (see f). Data is from NGDRC's (National Geophysical

(caption continued on previous page)

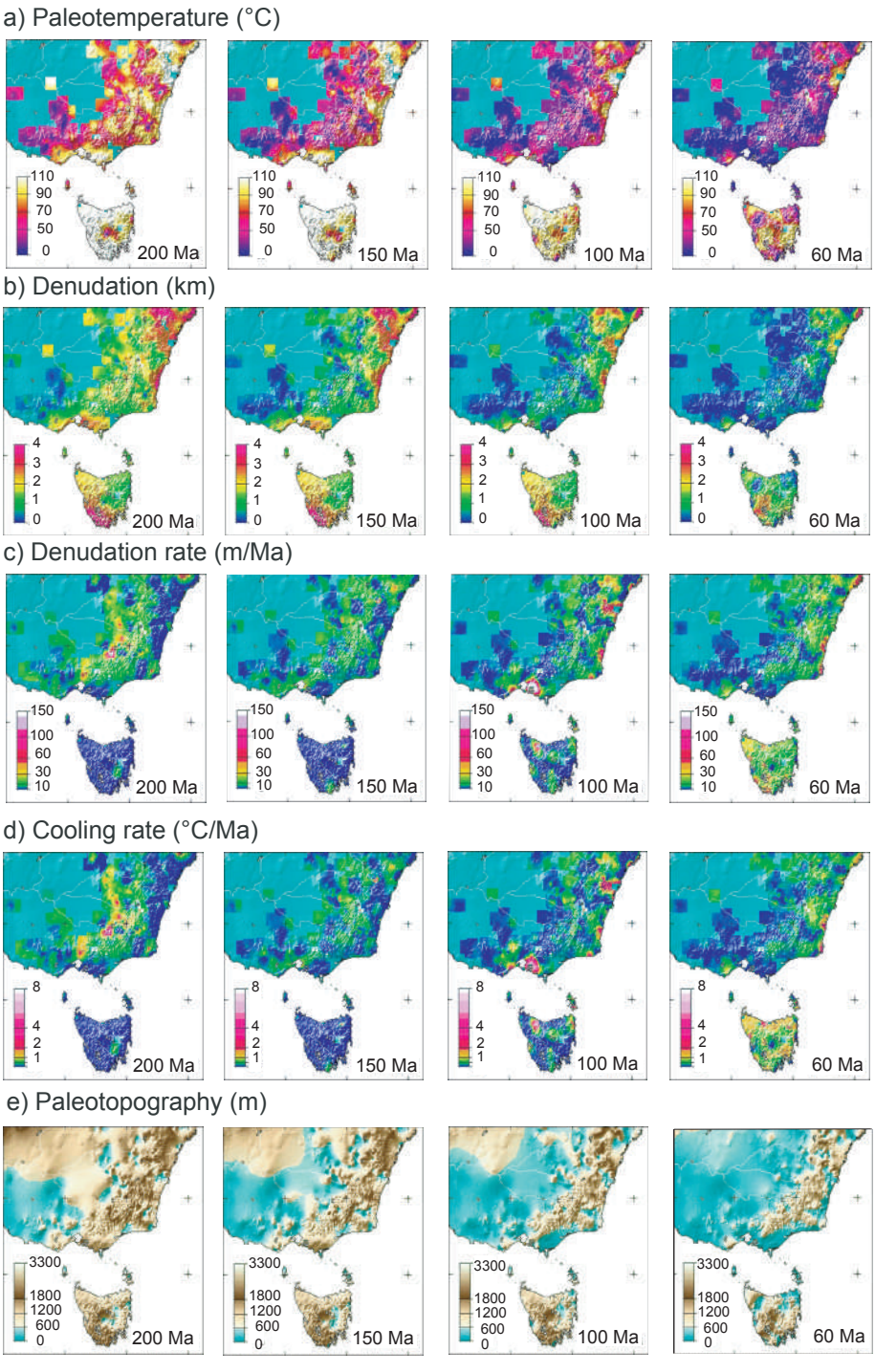

Plate IV. (caption on facing page)

pattern is burial under a sedimentary cover. We suggest that burial by foreland basin sediments shed from the Alleghenian Orogen has left a thermal imprint on the underlying southern Ontario shield rocks. The thickness of the sediments was sufficient to totally reset the AFT clocks (>~110 °C) in most of the Grenville Province. The thickness however rapidly decreased away from the orogen towards the north, resulting in only partial annealing of shield rocks on the southwestern flank of the Severn Arch, north of Lake Huron and east of Lake Superior. Along the Fraserdale Arch, and to the north of Lake Superior, no discernable thermal effect by the proposed burial is recorded by the AFT data.

In summary, the entire transect across the Canadian Shield in Ontario records a Paleozoic heating-cooling event, at least for the eastern half of the province, where the modeled time-temperature paths are well constrained. This heating is most likely associated with burial under sedimentary cover related to the Taconic orogeny, which remains preserved in outliers on the shield. The thermal signature of this event is progressively overprinted in the southeast Ontario shield by later burial under Alleghenian foreland sediments. No evidence for thermal effects related to the Acadian orogeny has been observed. This may reflect the possibility that none ever existed, that they are too subtle to be differentiated within the limits of modeling precision or that the effects of later thermal overprinting has removed such a record. It is very likely however, that large parts of the shield remained buried beneath a sheet of sediments throughout the Paleozoic and parts of the Mesozoic, as also implied independently by the work Patchett et al. (2004).

Southern Africa – formation and evolution of a continental interior

Geological overview. The pre-break-up geological evolution of southern Africa was dominated by the development of the Paleozoic-Mesozoic Karoo Basin. The Karoo Basin in South Africa formed as an extensive foreland basin ahead of the Cape Fold Belt (CFB) during the Early Permian (Tankard et al. 1982; Söhnge and Hälbich 1983). Thick sedimentary sequences accumulated along the southern margin of the CFB, but the sequence thins rapidly northwards forming a relatively thin cover (c. 1–2 km) over the Archaean and Proterozoic basement rocks in the cratonic interior. Remnants of the Permian Dwyka Formation tillites (basal Karoo) occur in exhumed paleovalleys where they underlie elevated river terraces (Martin 1953, 1973). These glacial deposits and striated bedrock surfaces, such as those exposed at Nooitgedagt (near Kimberly, South Africa), indicate that the present land surface represents an exhumed Permo-Carboniferous landscape in places (Visser 1987, 1995). The Clarens Formation aeoliantites (top Karoo) in South Africa (Dingle et al. 1983) have a maximum thickness of 300 m in the upper Orange River valley, but are generally about 100 m thick. This unit indicates terrestrial, semi-arid paleoclimatic conditions across southwestern Gondwana from the latest Triassic to earliest Cretaceous. Sedimentation within the Karoo Basin was terminated abruptly by the eruption of voluminous and extensive lavas of the Karoo continental flood basalts (~183 Ma) and the Paraná-Etendeka CFB (~132 Ma), which are up to 1.4 km thick in places (Erlank et al. 1984; Hawkesworth et al. 1992; Renne et al. 1996). After eruption of the Paraná-Etendeka flood basalts the surface geology is dominated by the thin (generally <200 m) Kalahari basin, which covers much of central southern Africa (Thomas

Plate IV (*on facing page*). Images showing the reconstructed paleotemperatures experienced by rocks now at the surface, their cooling rate, amount of denudation, rate of denudation and an estimated reconstruction of paleotopography for southeastern Australia for four separate time-slices; Early Jurassic (200 Ma), Late Jurassic (150 Ma), mid Cretaceous (100 Ma) and Paleocene (60 Ma). Paleotopography is based on "back-stacking" the present topography using the digital elevation data with the estimated amount of denudation and adjusting for an effective elastic thickness (Te) of 25 km (see Fig. 3; Gallagher and Brown 1999a; Gleadow and Brown 2000). See also caption for Late III for information on contouring procedure. Note samples from the Murray Basin area (Fig. 9) have not been included for generation of the image.

and Shaw 1990). The age of the base of the Kalahari basin sequence is thought to be Late Cretaceous to earliest Tertiary (Ward 1988; Thomas and Shaw 1990; Partridge 1993).

Continental break-up. Continental rifting between South America and Africa began during the Middle Jurassic (~150 Ma) (Nürnberg and Müller 1991). The rifting seems to have propagated south from the Falklands Agulhas fracture zone northwards towards the Walvis Ridge-Rio Grande Rise. The oldest magnetic anomaly clearly identifiable on oceanic crust on both the African and South American plates is M4 (130 ± 1 Ma), while further north near the Walvis Ridge the oldest identified anomaly is M0 (~125 Ma). Continental break-up was accompanied by syn- and post-breakup reactivation of pre-existing basement features such as the Central African and Mwembeshi shear zones (Coward and Potgieter 1983; Coward and Daly 1984; Daly et al. 1989) and involved significant intraplate deformation within west, central and southern Africa (Fairhead 1988; Unternehr et al. 1988; Fairhead and Binks 1991; Binks and Fairhead 1992; Brown et al. 2000). This later period of intracontinental deformation has been ascribed to shear stresses related to major changes in the geometry and relative motions of the plates involved in the opening of the Central and South Atlantic ocean basins.

Although rifting began in the Middle Jurassic and break-up finally occurred during the Early Cretaceous the major volume of sediment within the Orange and Walvis basins was deposited during the Late Cretaceous-early Tertiary (Brown et al. 1995; Rust and Summerfield 1990). Rust and Summerfield (1990) determined that this volume of ~2.8×10^6 km^3 (adjusted to equivalent rock volume) is equivalent to an average depth of denudation of 1.8 km over the whole of the Orange River catchment (an area of 1.55×10^6 km^2). The sedimentary record in the offshore basins clearly indicates that the continent has experienced very significant amounts of denudation (an average of 1.8 km) since the Middle Jurassic-Early Cretaceous. However, the chronology and spatial distribution of onshore denudation are likely to have been highly variable, depending on the post break-up tectonics, the pattern of drainage development, style of landscape evolution, lithological heterogeneity and long-term climatic variations.

Fission track results. A substantial set of AFT data (several hundred samples in total) has been collected from southern Africa. While the coverage is still sparse over large areas, the available data do provide some important new insights into the timing and distribution of long-term denudation at a sub-continental scale. The stratigraphic ages of samples analyzed range from Precambrian (Namaqua metamorphic belt) to Late Triassic (Stormberg Group, Upper Karoo Sequence). Despite this wide range of stratigraphic ages virtually all samples analyzed yielded AFT ages ranging between 166 ± 6 Ma and 70 ± 5 Ma (i.e., Cretaceous), with a conspicuous lack of younger AFT ages. AFT ages predating break-up at ~134 Ma were only obtained from samples in the interior regions of the continent and at elevations in excess of ~1500 m. Significantly, however, this is not a general characteristic of the continental interior, as some of the youngest ages (~70 Ma) were obtained from samples 600 km inland. AFT ages generally increase systematically with increasing elevation for specific localities.

The fact that all of the AFT ages are significantly younger than the stratigraphic age of the host rocks indicates that all the sampled rocks have been subjected to substantially higher temperatures in the past (mostly >~110 °C). Almost all the samples with Cretaceous AFT ages have mean confined track lengths >~12.5 to ~13 μm. The distributions of track lengths within these samples are generally unimodal with the mode between ~13 and 14 μm, and are generally negatively skewed with "tails" of shorter tracks (<~10 μm). This shows that most of the tracks have experienced only a moderate degree of thermal annealing (shortening) at temperatures <~70 °C. The majority of the samples must therefore have cooled from maximum paleotemperatures close to or greater than ~110 °C during the Cretaceous.

Quantitative images. Here we assumed that the eroded rock had an average thermal conductivity of 2.2 $W \cdot m \cdot K^{-1}$ and used surface heat flow data from Brazil and southern

Africa (Pollack et al. 1993) to derive estimates of the near surface temperature gradient. This approach accounts for spatially varying thermal gradients. Temporally varying heat flow and conductivity values, as derived from an independent thermal model for continental rifting for example, could easily be incorporated into the methodology but have not been in this paper.

In Plate IIa, we present maps showing the estimated paleotemperature at three times, 150 Ma, 90 Ma and 30 Ma of rocks presently outcropping on the surface. The earliest time broadly represents the time of continental break-up around southern Africa. For regions covered by the Late Cretaceous-Tertiary Kalahari basin sediments within southern Africa (Thomas and Shaw, 1990) paleotemperatures were set to the surface temperature during periods of deposition. The paleotemperature estimates were converted to equivalent depth as described above and maps representing the amount of denudation for each time are shown in Plate IIb and the estimated paleotopography in Plate IIc.

Thermotectonic history. At a regional scale the long-wavelength geomorphic response to continental rifting and break-up, indicated by the chronology and magnitude of denudation, varied significantly along the margins. For example, the substantial amounts of post-rift denudation indicated for the southwestern African margin probably reflects the geometry and timing of post-rift tectonic reactivation of major intracontinental structures (e.g., Raab et al. 2002). Overall the AFT data from southern Africa are consistent with models of landscape development which predict a major phase of denudation following continental rifting (e.g., Kooi and Beaumont 1994; Gilchrist et al. 1994; Brown et al. 2002). The chronology and rates of denudation inferred from the AFT results are also broadly similar to estimates derived from the offshore sedimentary record (Brown et al. 1990; Rust and Summerfield 1990). However, the timing and distribution of denudation is not compatible with simple escarpment retreat models following break-up, which predict only moderate amounts ($\leq$~1 km) of post-rift denudation inland of the margin escarpments. This is particularly true for southwestern Africa, and is partly a consequence of the post break-up tectonic history of the continental interior. A possible explanation of this discrepancy is that discrete tectonic episodes, inferred to have occurred during the Late Cretaceous and which included reactivation of major intracontinental structures, caused locally accelerated phases of denudation to be superimposed on the secular regional pattern. Alternative explanations for the observed pattern and history of denudation across the sub-continent which incorporate the recently documented dynamic uplift history of the African Superswell (e.g., Lithgow-Bertelloni and Silver 1998; Gurnis et al. 2000; Conrad and Gurnis 2003; Behn et al. 2004) during Cretaceous-Tertiary time will likely provide a more complete explanation for the spatially and temporally variable geomorphic history as documented using the regional imaging approach to analyzing thermochronologic data sets.

Eastern Africa – development of an intracontinental rift system

Geological overview. The crustal-scale mobile belts in East Africa formed during different Precambrian and early Paleozoic orogenic episodes (Shackelton 1986; Muhongo 1989; Stern 1994; Noble et al. 1997). Following the latest of these events, the Pan-African (~900−550 Ma), eastern Africa underwent a period of relative quiescence. This resulted in a phase of extensive peneplanation (Stagman 1978; Wopfner 1986), which was finally disrupted in Late Carboniferous-Early Permian time when the embryonic motions of the break-up of Gondwanaland commenced and sediments started to accumulate in basins of eastern Africa (e.g., Stagman 1978; Lambiase 1989; Kreuser et al. 1990; Wopfner and Kaaya, 1991).

The subsequent Phanerozoic geological history of eastern and central Africa has been dominated by continental extension (Daly et al. 1989; Lambiase 1989). This process has strongly influenced the regional geomorphology and led to the formation of widely recognized rift basins throughout East Africa (Reeves et al. 1987; Fairhead 1988; Daly et al. 1989; Lambiase 1989). It is also well documented that many post-Proterozoic faults that define these

basins and adjacent horst blocks were formed by the reactivation of pre-existing structures in the mobile belts (e.g., Gregory 1896; Smith and Mosley 1993; Smith 1994).

In Jurassic time the development of a triple junction centred on what is now the Lamu Embayment (Fig. 7) led to seafloor spreading between Africa and Madagascar and the development of the East African passive margin (Reeves et al. 1987). The Anza Rift, which extends northwest from the Lamu Embayment as far as Lake Turkana (Fig. 7), is the failed arm of this Jurassic triple junction (Reeves et al. 1987). The Anza Rift was periodically reactivated with major periods of extension and sedimentation in the Early and Late Cretaceous and continuing through to Oligocene time (Reeves et al. 1987; Greene et al. 1991; Bosworth and Mosely 1994). The Cretaceous extensional episodes marked the eastern limit of intracontinental deformation in the west and central African rift system, which forms a series of rift basins and transform faults that developed in response to differential movement between continental fragments during opening of the South Atlantic Ocean (Fairhead 1988; Daly et al. 1989). Each of the rifting episodes in the Anza Rift led to regionally extensive erosional denudation of basement rocks in East Africa (Foster and Gleadow 1992a, 1993a, 1996; Noble et al. 1997).

In Late Oligocene to Early Miocene time, extension related to the Kenya Rift began in north Kenya (e.g., Morley et al. 1992). The present morphology of the Kenya Rift itself is a result of continental extension that has been taking place from Miocene to Recent times (Baker et al. 1972). A nascent continuation of the eastern branch of the East African Rift System, which represents an initial stage of development for a propagating rift, is observed in eastern Tanzania (Fig. 7). Some of the present topography and structural architecture of the Kenya Rift area is probably related to older rifts, such as the Anza Rift and Lamu Embayment (Reeves et al. 1987).

Fission track results. Over 430 AFT ages have been determined across eastern Africa and these are reported in several studies (Gleadow 1980; van den Haute 1984; Wagner et al. 1992; Foster and Gleadow 1992a, 1993a, 1996; Mbede et al. 1993; van der Beek 1995; Eby et al. 1995; Noble 1997; Noble et al. 1997; van der Beek et al. 1998). About 350 of these results also have accompanying track length determinations and the localities for these samples are shown in Plate IIIa, along with the AFT data summarized in interpolated images presented in Plate IIIb-c. Sampling strategies varied according to the particular study, but where quantitative images were constructed (Plate IIIe-f) most samples used were based on data reported by Foster and Gleadow (1992a, 1993a, 1996), Noble (1997) and Noble et al. (1997). These samples were mainly derived from suites collected systematically with elevation or across important structural blocks and regional trends, and also sampled to provide insights into the low temperature thermal effects of rift propagation and the response of cratonic crust during Phanerozoic rifting episodes (Plate IIIa).

AFT ages are generally <250 Ma, with two prominent groupings (Plate IIIb): <100 Ma along the coastal area and in northern Kenya and ~100 to 250 Ma inland in Kenya (E39°:S5° and E37°:N4°), Tanzania (E35°:S7°), Rwanda (E30°:S9°) and northern Zimbabwe (E30°:S16°). The youngest ages (≤50 Ma) are confined to the margins of Phanerozoic basins, i.e., the Anza Rift of Kenya (E34°:N4° to E40°:S4°), and the western branch of the East African rift system in southern Tanzania (E34°:S9°), and Malawi (E36°:S15°). The oldest ages (>300 Ma) are generally restricted to the Tanzanian craton of central Tanzania and southwestern Kenya (E33°:S5°).

There are two significant departures from this general pattern. Firstly, AFT ages in Burundi, adjacent to the western branch of the East African rift system and adjacent to Lake Rukwa in southwestern Tanzania are significantly older than any other samples lying in proximity to extensional basins. Secondly, one AFT age on the eastern margin of the

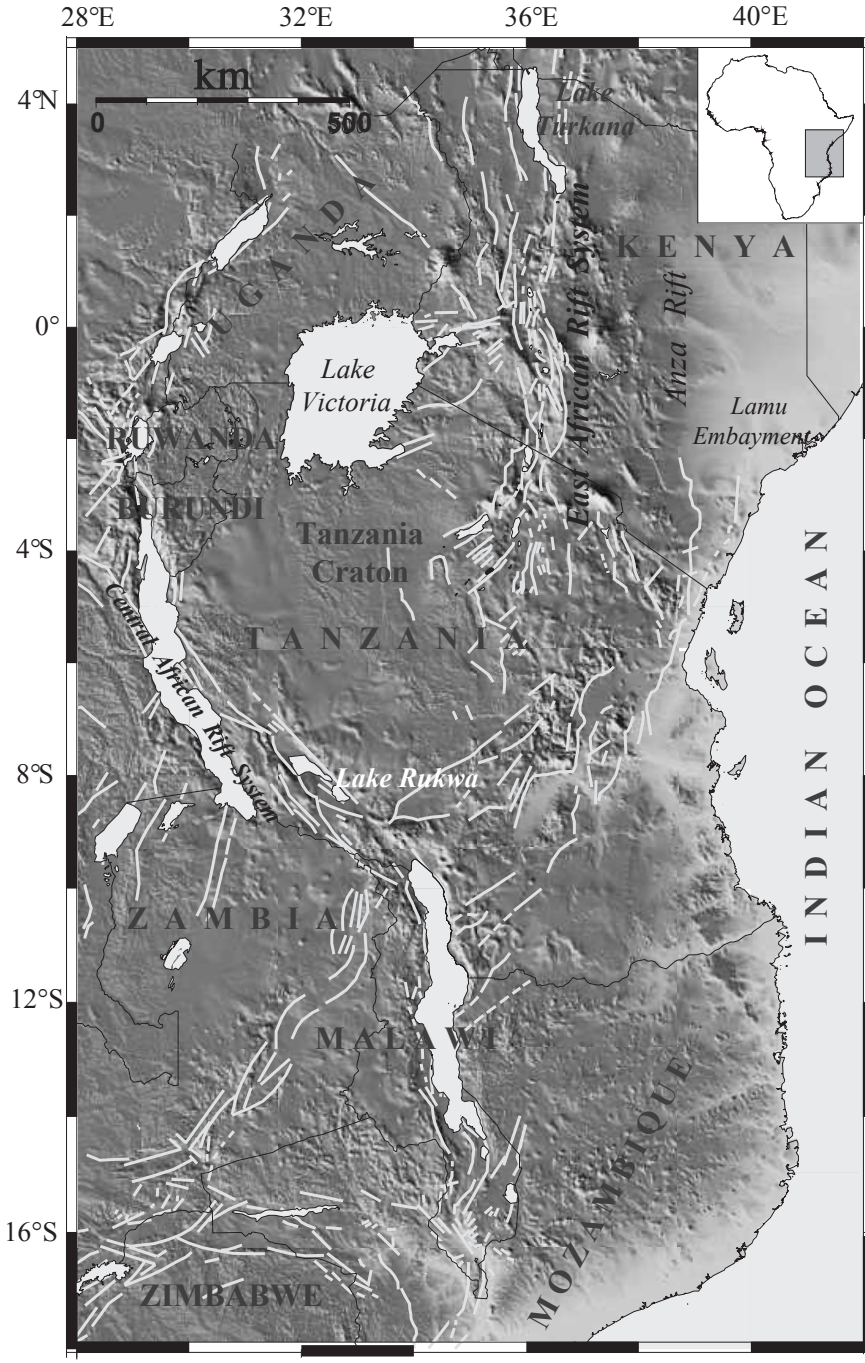

Figure 7. Locality map of eastern Africa showing topography, some geological elements and faults (in white), which are related to Phanerozoic rifting (faults after Rosendahl 1987), generated using GMT-3, version 3.0 (Wessel and Smith 1991). Shaded topography uses the 30′ DEM from the US Geological Survey EROS Data Centre.

Tanzanian craton (E35°:S6°) yields a significantly younger age (~60 Ma) compared to all other cratonic samples.

In addition, the range of AFT ages can also be linked with changes in elevation. In general, youngest ages are found at lowest elevations, i.e., the coastal region (~35 to70 Ma) and increase towards the higher elevations of the continental interior (375 to 400 Ma).

Mean HCTL range predominantly between 12 to 13 μm (Plate IIIc). A smaller number of samples located along the flanks of the Anza Graben, in isolated areas on the Tanzanian craton and in southern Malawi yield longer mean HCTL between 13 to 14 μm. The lowest mean HCTL (~11 μm) are found in areas adjacent to the east-bounding fault of the Tanzania Craton, and in southeastern Kenya. The regional pattern of HCTL also appears to vary with elevation showing a decrease away from low-lying coastal areas (~13 to 14 μm) towards the higher interior of the continent (12–13 μm).

Quantitative images. The evolving temperature history of samples from eastern Africa is shown in Plate IIIe. Regional modeling suggests that during Early Jurassic time (180 Ma) rocks currently exposed along the eastern margin of the sampled area and northeastern margin of the Zimbabwe Craton (E30°:S16°) were at temperatures of >110 °C. It is important to note that modeling parameters have a predefined upper default value of ~110 °C, thus until samples record cooling below this temperature the modeling protocol assigns a value of 110 °C. By 180 Ma samples on the eastern margin of the craton (E35°:S7°), in SW Kenya (E36°:S1°), southern Tanzania (E34°:S9°), and northern Zimbabwe (E30°:S16°) had cooled to below ~80 °C. At the same time, some areas of southwest Kenya (E35°:S1°) and central Tanzania (E34°:S4°) are predicted to have cooled to surface temperatures. Prior to the Early Jurassic the information provided by AFT data is limited and only the oldest rocks exposed in the western portion of the sample area were at or below 110 °C.

During the period between 180 Ma and 90 Ma cooling continued, most notably around central Tanzania and southwestern Kenya, expanding the area over which rocks had cooled below ~100 °C. Also during this time interval the eastern margin of the study area and around the Malawi rift (E34°:S10°) does not appear to have undergone any cooling. This area most likely underwent some cooling at this time but remained at a temperature >110 °C. The cooling history between middle Cretaceous and the middle Tertiary (90 to 30 Ma) is much more pronounced along the coastal region, with a significant number of samples cooling more rapidly from >~110 °C to <80 °C. At the same time the samples from southwestern Kenya (E35°:S1°) and central Tanzania (E34°:S4°) underwent more subdued cooling. By 30 Ma most rocks in the study area were close to surface temperatures however a number of important exceptions in Kenya (E35°:N4°, E38°:N1°and E39°:S4°) and central Tanzania (E35°:S6°) suggest that some areas have undergone significant cooling in the last 30 Ma.

As shown previously, thermal histories can be used to estimate the amount and timing of denudation if a paleothermal gradient, paleosurface temperature and rock conductivity of the removed section is assumed (see also Fig. 3). It is noteworthy here that as the geothermal gradient varies across the area (Plate IIId) the resulting pattern of denudation will differ from the cooling histories shown in Plate IIIe (i.e., lower geothermal gradients result in higher estimates of the amount of denudation and vice-versa). The lowest geothermal gradients are found in Zimbabwe, central Tanzania and eastern Kenya, whereas the areas adjacent to rift margins have higher estimates. Time-slices for the denudation history of samples collected in eastern Africa are shown in Plate IIIf.

Areas in southwestern Kenya (E35°:S1°), central Tanzania (E34°:S4°) and Zimbabwe (E30°:S17°) are predicted to have had ~2 to 4 km of section removed since Late Jurassic time while the same areas experienced only 1 to 2 km of denudation since the mid Cretaceous (Plate

IIIf). By contrast, the coastal region of eastern Africa appears to have undergone ~6 km of denudation over the last 90 Ma.

Thermotectonic history. Previous geochronology studies for exposed rocks in eastern Africa generally yield Precambrian ages and therefore do not provide direct information on events occurring over the past ~500 Ma of geological history (e.g., Frisch and Pohl 1986; Munyanyiwa 1993; Möller 1995). The AFT data however, provide tectonothermal information for this significant time period. The range and distribution of AFT parameters across eastern Africa indicate that the Phanerozoic regional history is complex and closely related to the development and reactivation of sedimentary basins (e.g., Foster and Gleadow 1992a, 1993a, 1996). Another important feature is that the fission track parameters determined for the Precambrian mobile belts and Archaean cratons (Tanzanian and northern Zimbabwe) are, at least in some areas, remarkably similar. This suggests that these areas also share segments of a common Phanerozoic low temperature thermal history.

AFT data show that the post Pan African development of eastern Africa was characterized by long periods of slow cooling punctuated by at least four accelerated cooling events, commencing in Triassic (>220 Ma), Early Cretaceous (~140−120 Ma), Late Cretaceous-Early Tertiary (~80−60 Ma) and Middle to Late Tertiary time (Wagner et al., 1992; Foster and Gleadow, 1992a, 1993a, 1996; Mbede et al., 1993; van der Beek, 1995; Noble 1997; Noble et al., 1997). For the most part the relatively rapid cooling is interpreted as resulting from episodes of increased denudation related to the formation and reactivation of high angle fault blocks that moved in response to intraplate stresses. The episodes of denudation are also broadly contemporaneous with the deposition of packages of clastic sedimentary rocks in the basins of eastern Africa (Fig. 8). The periods of relatively rapid cooling are likely to be due to denudation at rates >30 m/Ma because of the preservation of relatively long mean track lengths. The actual rates of denudation probably ranged between 30 to 100 m/Ma during episodes of

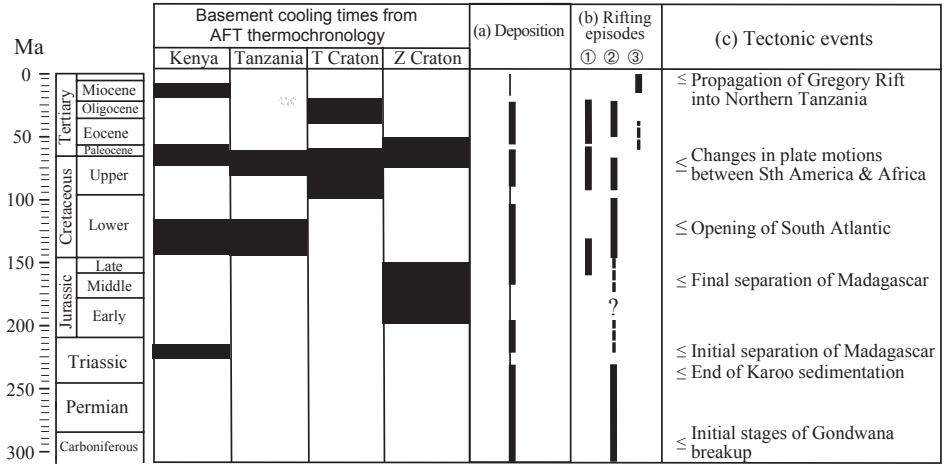

Figure 8. Comparison of periods of rapid denudation/cooling and fault reactivation revealed through AFT studies in Eastern Africa, with periods of: (a) sediment deposition into East African basins; (b) rifting episodes in the Anza Rift, Central African Rift System and East Africa Rift System; (c) regional tectonic events (modified after Winn et al. 1993). Periods of accelerated cooling defined from AFT thermochronology studies (Foster and Gleadow 1992a, 1993a, 1996; Noble 1997; Noble et al. 1997). Thick lines for deposition and rifting episodes denote time periods when both rate and style of sedimentation changed as a result of periods of rifting). T Craton = Tanzania Craton, Z Craton = Zimbabwe Craton (modified after Noble 1997 and Noble et al. 1997).

accelerated erosion (over periods of 10 to 20 Ma) and <5 m/Ma for the intervening times. This calculation is based on age versus elevation gradients and the timing of model histories and the geothermal gradients (Foster and Gleadow 1992a, 1993a, 1996; Noble 1997).

The last two episodes appear to be regionally more extensive. In most cases this is due to the removal of evidence for the older events by later denudation during the younger events. This is especially true for areas adjacent to the younger rifts, e.g., southeast coastal Kenya. The prominence of the last episode during Middle to Late Tertiary may also have been influenced by the regional interaction of plumes in eastern Africa during the later part of the Phanerozoic.

During Phanerozoic rifting in eastern Africa, it has previously been assumed that the Tanzanian and Zimbabwe Cratons have remained relatively inert (e.g., Muhongo 1989; Rach and Rosendahl 1989). The quantitative images however, clearly show that this is not the case and that periods of accelerated denudation and fault reactivation punctuated the tectonothermal history of the cratons at least since Mesozoic time (Plate IIIf) and even earlier (Noble et al. 1997). The timing of periods of denudation and fault reactivation are related to the tectonic evolution of East Africa and are contemporaneous with tectonic reactivation in the adjacent structural belts.

Southeastern Australia – evolution of a complex rifted passive margin

Geological overview. During Paleozoic to mid Cretaceous time, Australia, Antarctica and New Zealand were joined together in eastern Gondwanaland. Throughout much of this time eastern Gondwanaland was a convergent plate margin whose architecture was shaped mainly by its convergence with oceanic plates driven from the Pacific region (Veevers 1984). As a result the Paleozoic fold belts and basins of eastern Australia record a series of subduction-related deformational events. These include Early to Middle Paleozoic episodes responsible for formation and deformation of the Lachlan Fold Belt (Veevers 1984; Coney et al. 1990; Fergusson and Coney 1992; Gray 1997; Foster and Gray 2000) and the Late Permian to Early Triassic episodes which created the New England Fold Belt (Fig. 9) to the north and east (e.g., Harrington and Korsch 1985). The Lachlan Fold Belt is characterized by early to middle Paleozoic rocks including metamorphosed Cambrian through Devonian (primarily Ordovician) volcanic and cratonic-derived deep marine sedimentary rocks and extensive Early Silurian, Early Devonian and Late Carboniferous granitic rocks. By the Early to Middle Carboniferous all regional deformation within the Lachlan Fold Belt had ceased (Foster and Gray 2000).

The New England Fold Belt is composed predominantly of the deformed and metamorphosed remnants of an accretionary complex initially formed during Late Devonian-Early Carboniferous time. By the Late Carboniferous an extensional tectonic regime became predominant and numerous synkinematic S-type granites were intruded, mostly into the lower crust. Extension had ceased by the Late Permian and a major thrust-dominant contractional deformational event (Hunter-Bowen Orogeny) occurred accompanied by the intrusion of significant volumes of Late Permian to Triassic magma (Collins 1991). The Sydney Basin is a foreland basin overlying basement rocks, in part consisting of the Lachlan Fold Belt to the west and the New England Fold Belt to the north (Fig. 9). Subsidence and deposition and subsidence in the basin of a thick sequence of marine and non-marine sediments commenced in the Early Permian and continued through to the Jurassic, with a possible hiatus in the Late Triassic (Mayne et al. 1974). Permian sedimentary rocks within the Sydney Basin were deformed during the Late Permian-Early Triassic Hunter-Bowen Orogeny.

In the Late Jurassic, extension between Australia and Antarctica initiated from west to east (Johnson and Veevers 1984; Norvick and Smith 2001), followed in the Early Cretaceous by rifting along the southern margin (Veevers et al. 1991). Break-up between the Australian and Antarctic plates subsequently occurred in the middle Cretaceous (~95 Ma) and is marked

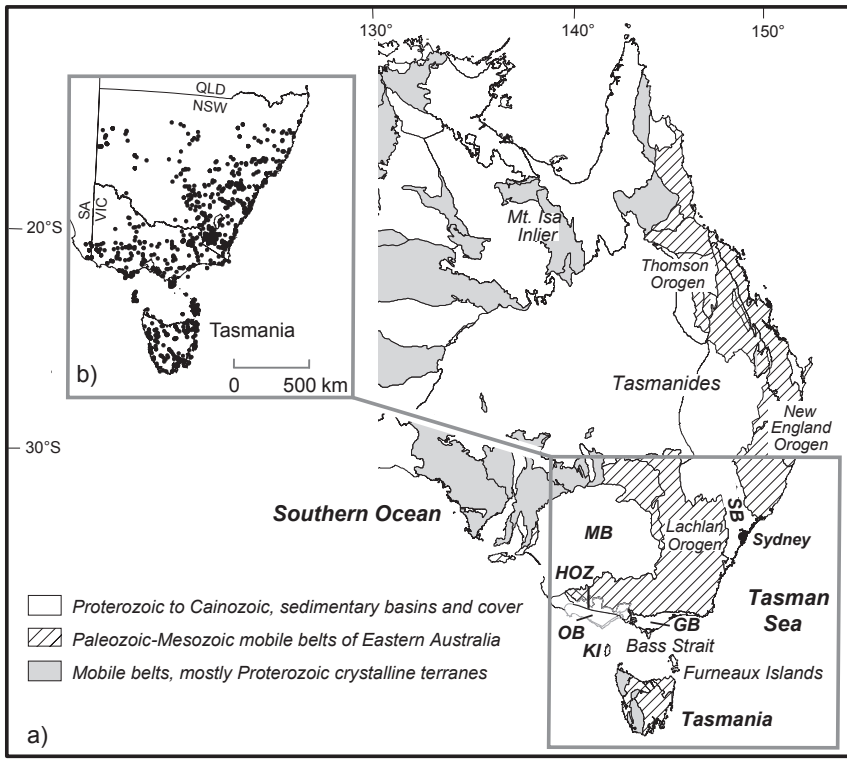

Figure 9. Locality and geological map of eastern Australia (modified after Palfreyman 1984) showing: (a) main crystalline terranes and grey inset delineating the southeastern Australia study area. Sedimentary cover, shown in white, was largely excluded from this study. Map (b) shows apatite fission track sample localities (~850) most of which were used for this study to construct the images shown in Plate IV. *GB* = Gippsland Basin, *KI* = King Island, *MB* = Murray Basin, *SB* = Sydney Basin, *HOZ* = hybrid orogenic zone (separating the Lachlan and Delamerian orogenic belts) and *OB* = Otway Basin.

by a major unconformity throughout the rift-related basins (Veevers 2000), e.g., Otway and Gippsland Basins located along the southern margin of Australia (Fig. 9a). However, the final separation to open the Southern Ocean did not propagate through Bass Strait, but was offset to the south of Tasmania. The magnetic anomalies in the Southern Ocean suggest that spreading was very slow until the Eocene (Cande and Mutter 1982; Veevers 2000). During the mid-Cretaceous (at ~105 Ma), subduction to the east of Australia ceased (Cande and Kent 1995). Subsequently, at ~100 Ma south- to north-directed continental rifting between Australia and the Lord Howe Rise/New Zealand began along what is now the eastern Australian margin. The timing of passive margin rifting along eastern Australia is well constrained by ocean floor magnetic anomalies and seismic data from the Tasman Sea rift (e.g., Weissel and Hays 1977; Veevers et al. 1991) which suggest spreading commenced at ~86 Ma and continued until ~62 Ma (Cande and Kent 1995). The onset of fast spreading in the Southern Ocean leading to the final separation of Australia and Antarctica in middle Eocene time is related to a significant global plate rearrangement (e.g., Cande and Mutter 1982). Structure and topography of the present-day southeastern margin are believed to be predominantly controlled by Late Mesozoic-Early Tertiary rifting, further details of which are summarized by Johnson and Veevers (1984) and Lister and Etheridge (1989).

Fission track results. Most samples for AFT studies were collected from exposed granitic rocks of the Paleozoic to Mesozoic mobile belts on the mainland, as well as in Tasmania and some offshore islands, which are part of the continuous continental crust (Fig. 9a). A small number were collected from basement rocks intersected in shallow borehole occurrences (<100 m depth) beneath shallow cover. In some areas samples included various metamorphic and sedimentary lithologies, and in Tasmania, Jurassic dolerites, but overall, some 90% of the samples studied are rocks of granitic composition with a relatively limited compositional range. AFT data from ~830 samples (see Fig. 9b) were judged to be of sufficient quality in both age and length data to be included in this study. Samples were excluded on the basis of having too few length measurements (<40) or too few grains counted (<6), or where obvious local geological disturbance, reflected in anomalous AFT data had occurred, such as by young volcanic activity.

Over the past ~25 years, several AFT studies have been carried out in areas bordering the southeastern continental margin (e.g., Gleadow and Lovering, 1978a,b; Moore et al. 1986; Dumitru et al. 1991; Foster and Gleadow 1992b, 1993b; O'Sullivan et al. 1995a,b, 1996a,b, 1999a,b, 2000a,b,c; O'Sullivan and Kohn 1997; Gleadow et al. 1996, 2002b; Kohn et al. 1999, 2002; Weber et al. 2004). Although the apparent AFT ages reported from these areas may range from mid-Paleozoic to Tertiary, they only rarely reflect the formation or depositional ages of the host rocks sampled, which are mostly of Paleozoic age. Further, the AFT data often show broad spatial variations that reflect their thermal and denudation histories. These have been interpreted in terms of a regional late Paleozoic cooling over the area modified by later cooling events associated with continental rifting and break-up on the eastern and southern margins (Dumitru et al. 1991; Gleadow et al. 1996, 2002b; Kohn et al. 2002). The most important regional AFT variations include:

1.) A tendency for the youngest ages ranging between ~50 to 100 Ma to be concentrated on and around the southeastern and eastern rifted margin of the continent. Many mean track lengths from these same areas are very long and often exceed 14 μm indicating that the apparent ages are actually dating the time of episodes of rapid cooling. Inland of the "young" age trend there is generally a belt of older ages and much reduced mean track lengths (<12.5 μm). Some of the individual length distributions for this region appear bimodal or unusually broad in character, indicative of mixed ages, intermediate between an older and younger value.

2.) A distinctly different pattern for Tasmania, south of the mainland, with ages across the island mostly <100 Ma and ranging between 30 and 250 Ma. Many of these young ages are also associated with long mean track lengths and narrow unimodal track length distributions, indicating that the ages reflect episodes of rapid cooling (O'Sullivan and Kohn 1997). Some older ages and shorter mean track lengths similar to those observed in the inland trend on the mainland are found in the centre of Tasmania and on King and the Furneaux Islands within Bass Strait (see Fig. 9a and O'Sullivan et al. 2000c).

3.) A relatively abrupt transition to much older ages (~300−400 Ma) in western Victoria going westwards along the southern margin of the mainland. This was first reported by Foster and Gleadow (1992, 1993) who suggested that the transition coincided approximately with the terrane boundary between the early Paleozoic Delamerian (to the west) and Lachlan orogenic belts (to the east) and reflected a change in the style of rifting along the southern margin to the west and east of a hybrid orogenic zone (Miller et al. 2004; also see Fig. 9a). The mean track lengths in the region of old ages are of generally intermediate values (12.5–13.5 μm) indicative of more prolonged cooling histories.

Southeastern Australia AFT age versus mean track length plots all show a characteristic "boomerang" trend with an upwards trend of longer track lengths to young ages (Gleadow et al. 2002b). This implies that the region has been widely affected by rapid cooling episodes with distinct differences in the timing of these rapid cooling episodes (defined by the track lengths clusters >14 μm) between different regions, with Victoria older than the remaining southeastern margin which in turn is older than Tasmania.

Quantitative images. Using the approach described above (see also Fig. 3) the southeastern Australia AFT data set has been modeled to construct quantitative paleotemperature, cooling rate, amount of denudation, denudation rate and paleotopography images as a function of time and space. A series of four time-slice images at 200 Ma, 150 Ma, 100 Ma and 60 Ma is presented in Plate IV. For the construction of the images we have used a spatially constant present day heat flow and surface temperature, and a constant thermal conductivity of 2.5 $Wm^{-1}K^{-1}$ (as used by Sass and Lachenbruch 1979 for the Eastern Heat Flow Province of Australia) to convert temperature to depth. It should be noted that samples from the Murray Basin area (Fig. 9b) were excluded in the construction of the quantitative images.

A remarkable feature of the time slice images presented is the sizeable area of present day surface rocks which were at paleotemperatures close to or greater than 110 °C at 200 Ma. Many of these areas had cooled to lower temperatures by 100 Ma, although parts of coastal eastern Australia and Tasmania still remained at relatively high temperatures into Early Tertiary time. In this analysis western Victoria stands out as one area where Paleozoic rocks have experienced relatively little thermal disturbance and have remained at relatively low temperatures since ~200 Ma (Plate IV).

Converting the paleotemperature data into denudation estimates and taking into account the assumptions described previously, suggests that cumulative denudation in most parts of the study region was between ~2–4 km since ≥200 Ma. In some mainland coastal areas and over much of Tasmania however, this amount of denudation was mainly achieved over the past ~60 Ma.

The visual pattern observed from the images displays clearly in time and space some of the main points arising from earlier studies, which indicate that since the end of orogeny, different regions of the mobile belt rocks of southeastern Australia record distinct episodes of accelerated denudation (e.g., O'Sullivan et al. 1996a, 2000b; Gleadow et al. 2002b; Kohn et al. 1999, 2002). Such reported episodes occurred during Late Permian to Early Triassic (~265–230 Ma), middle Cretaceous (~100−85 Ma) and Paleocene to Middle Eocene (~60−45 Ma) time.

Thermotectonic history. Late Permian to Early Triassic cooling in the Lachlan Orogen has been related to a far-field denudational response associated with the Hunter-Bowen Orogeny (e.g., O'Sullivan et al. 1996a, 1999a; Kohn et al. 1999, 2002). By contrast, later mid Cretaceous cooling may have been caused by the cessation of dynamic platform tilting due to subduction in early Late Cretaceous time (e.g., Gallagher et al. 1994a; Waschbusch et al. 1999). This would have resulted in rebound, leading to km-scale denudation. Added to this is the effect of contractional deformation (~90−95 Ma) associated with inversion and reactivation along the eastern margin of the continent and the onset of rifting in the Southern Ocean and Tasman Sea (Hill et al. 1995).

Van der Beek et al. (1999) analyzed the present day drainage pattern and denudation history of southeastern Australia and suggested that regional km-scale mid-Cretaceous uplift may not have taken place. Rather, they proposed that the observed cooling may have resulted from denudation related to base-level drops associated with rifting in the Bass-Gippsland basins to the south and the Tasman Sea to the east (Fig. 9a). The isolated occurrences of mid Cretaceous igneous rocks in southeastern Australia rule out the possibility that mid-

Cretaceous cooling may be the result of cooling following a period of elevated heat flow linked to a magmatic event (Kohn et al. 2003).

In general, coastal plain areas exhibit a greater amount of denudation than those inland. But the complex nature of events associated with continental break-up and the formation of new-rifted margins is highlighted by fact that times of rapid cooling may pre-date and postdate the actual time of seafloor spreading onset in the adjacent ocean basins (Plate IV).

The difference in timing of cooling episodes between different areas is also demonstrated by surface denudation rates through time presented for six specific sub-regions of southeastern Australia (Fig. 10). These may be equated with the volumes of sediment derived from the respective landscapes over the time intervals indicated and allow for the predictions to be tested by matching against the stratigraphic record of various sedimentary basins, provided these are preserved (e.g., Weber et al. 2004). It is emphasized that the regional denudation chronology estimates, derived by the integration of spatial denudation information for a particular time interval, produces the "locally-averaged" denudation rate for a specified region as a function of time. Hence, distinctive cooling patterns seen in some individual samples or in samples from a restricted area may not necessarily be highlighted prominently within the overall "average" regional denudation pattern.

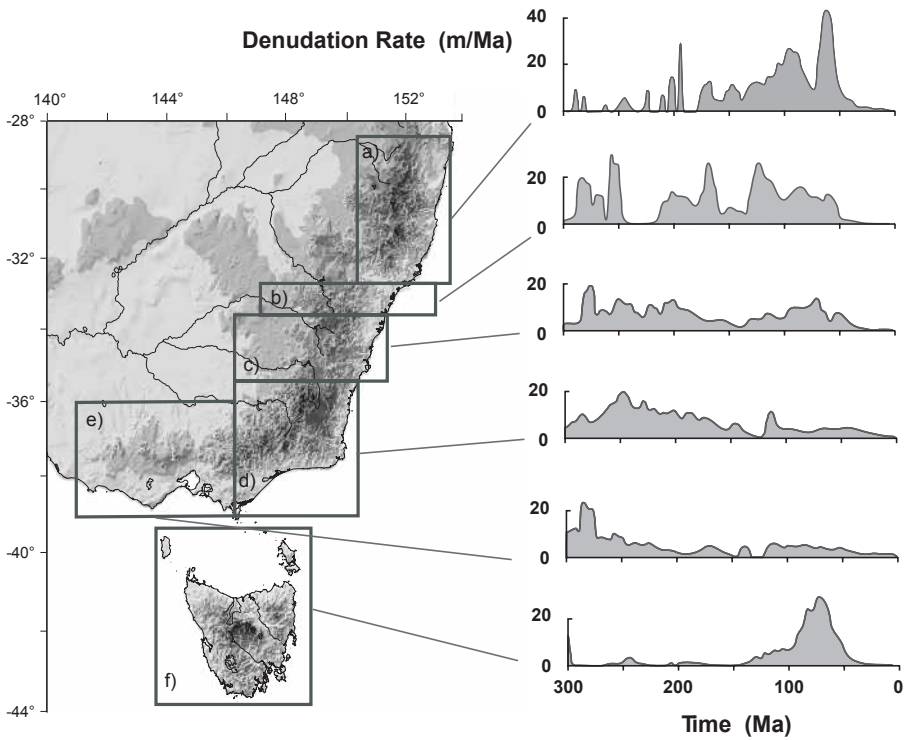

Figure 10. Long-term smoothed (spatially averaged) denudation chronology plots for six sub-regions (a to f) in southeastern Australia based on an initial track length of 14.5 μm. Note the marked differences in denudation history apparent across the different areas. Areas (a) and (f) show pronounced Cretaceous to Early Tertiary denudation, areas (b)-(d) show accelerated denudation in Late Paleozoic-Early Triassic time, whereas area (e) shows particularly low rates of denudation from Mesozoic to Present (see text for further discussion).

Tasmania shows a markedly different and significantly younger cooling history to the mainland. The denudation chronology for Tasmania reveals a steady increase in Early Cretaceous time to a maximum peak in mid Paleocene to mid Eocene time and then a decrease to the Present (Figs. 2b and 10). This is indicative of its continued tectonic emergence and denudation throughout much of the Cenozoic and probably reflects the proximate position of Tasmania, with its very narrow continental shelves and the evolving rift systems between Australia and Antarctica and the Lord Howe Rise/New Zealand.

CONCLUDING REMARKS

AFT thermochronology is a well-established tool for reconstructing the low temperature thermal and tectonic evolution of the continental crust. From the earliest studies of continental terranes it has been apparent that AFT data show broad regionally consistent patterns of variation. The variations are primarily controlled by cooling, which may be initiated by earth movements and denudation at the Earth's surface and/or by changes in the thermal regime. As such the data frequently bear little or no relationship to the original formation ages of the rocks involved. However, the significance of the regional patterns is not always obvious and there have often been difficulties in interpreting and integrating the results of such studies with other sets of geological observations. Using numerical forward modeling procedures the measured AFT parameters can be matched with time-temperature paths using an optimal data fitting procedure, which enables thermal and tectonic processes to be mapped out in considerable detail. Large regional arrays of data can be modeled sequentially and inverted into time-temperature solutions for visualizing the evolution of paleotemperatures, denudation rates and paleotopography of present day surface rocks. These can then be viewed as a series of time-slice images and the regional spatially integrated denudation rate chronology. The images provide a striking new quantitative perspective on crustal processes and landscape evolution and allow important tectonic and denudation events over time scales up to hundreds of million years to be readily visualized in a variety of ways and integrated with other regional data sets such as digital terrain models, heat flow, etc. This approach provides a readily accessible framework for quantifying the often undetectable, timing and magnitude of long-term crustal denudation in many terranes, for a part of the geological record often largely unconstrained.

The images are not only valuable for visualizing the thermochronological information but also allow a new range of quantitative measurements to be made on the virtual landscapes constructed. For example, a direct consequence of the denudation models is to predict sediment volumes and to trace the evolution of drainage basins, at least on a broad scale. This opens up the possibility of making a new range of mass-balance calculations on the amounts and nature of eroded material and sediment accumulation in appropriate depocenters (e.g., Weber et al. 2004). Similarly, predictions of long-term surface denudation rates can be tested against more recent estimates based on cosmogenic isotope analyses (e.g., Belton et al. 2004), at least for the most recent part of the record. The acquisition of apatite (U-Th)/He data (e.g., Farley 2002) on a similar regional scale should provide more robust information on the lower temperature portion of the thermal history (<~60−70 °C), which is poorly constrained by AFT data. In addition, information derived from higher temperature thermochronometric systems e.g., $^{40}Ar/^{39}Ar$ K-feldspar (McDougall and Harrison 1999; Harrison et al. 2005), (U-Th)/He zircon and titanite (Reiners and Farley 1999; Reiners 2005) and zircon fission track (Tagami 2005) could potentially also be integrated into imaging schemes, providing for a more comprehensive visualization of intermediate to low temperature thermal histories.

With increasingly large AFT datasets from regional studies becoming available it will be necessary to make data collection more efficient. One promising direction in this regard is through emergence of Laser-Ablation-Microprobe Inductively Coupled Plasma Mass

Spectrometry (LAM-ICP-MS). This approach allows for the analysis of trace elements in small areas (10−30 μm) within mineral grains and has opened the way to a radically different approach to fission track analysis that does not require neutron irradiation for the analysis of uranium content (Hasebe et al. 2004). As such LAM-ICP-MS promises a drastic reduction in sample turn-around time and improved laboratory safety due to the elimination of the need for neutron irradiations, a requirement, which now imposes relatively long delays on sample processing.

ACKNOWLEDGMENTS

The Australian Research Council, the Australian Institute of Nuclear Science and Engineering, and the former Australian Geodynamics Cooperative Research Centre funded this research. We acknowledge the various contributions of many colleagues related to the acquisition of regional fission track data sets, particularly former members of the fission track groups at the School of Earth Sciences at La Trobe University and more recently at the University of Melbourne, particularly to Paul O'Sullivan, David Foster and Asaf Raza. We are also grateful to Kirk Osadetz and Richard Everitt for their assistance in acquiring samples for the Canadian data set. We thank Paul Andriessen, Geoff Batt, Ann Blythe and Tim Carter for their helpful reviews of this chapter.

REFERENCES

Baker BH, Mohr PA, Williams LAJ (1972) Geology of the Eastern rift system of Africa. Geol Soc Am Spec Paper 136:1-67

Barbarand J, Carter A, Wood I, Hurford A (2003) Compositional and structural control of fission-track annealing in apatite. Chem Geol 198:107-137

Behn MD, Conrad CP, Silver PG (2004) Detection of upper mantle flow associated with the African Superplume, Earth Planet Sci Lett 224:259-274

Belton DX, Brown RW, Kohn BP, Fink D, Farley KA (2004) Quantitative resolution of the debate over antiquity of central Australian landscapes and implications for the tectonic and geomorphic stability of cratonic interiors. Earth Planet Sci Lett 219:21-34

Binks RM, Fairhead JD (1992) A plate tectonic setting for the Mesozoic rifts of West and Central Africa. Tectonophys 213:141-151

Bosworth W, Morley CK (1994) Structural and stratigraphical evolution of the Anza rift, Kenya. Tectonophys 236:93-115

Bray RJ, Green PF, Duddy IR (1992) Thermal history reconstruction using apatite fission track analysis and vitrinite reflectance: a case study from the UK East Midlands and the Southern North Sea. *In:* Exploration Britain: Into the Next Decade. Hardman RFP (ed) Geol Soc Lond Spec Pubs 67, p 3-55

Brown LF Jr, Benson JM, Brink GJ, Doherty S, Jollands A, Jungslager EHA, Keenen JHG, Muntingh A, van Wyk NJS (1995) Sequence Stratigraphy in Offshore South African Divergent Basins. An Atlas on Exploration for Cretaceous Lowstand Traps, Soekor (Pty) Ltd, Am Assoc Petrol Geol Studies in Geol 41, 184 p

Brown RW (1991) Backstacking apatite fission track "stratigraphy": a method for resolving the erosional and isostatic rebound components of tectonic uplift histories. Geology 19:74-77

Brown RW, Summerfield MA (1997) Some uncertainties in the derivation of rates of denudation from thermochronologic data. Ear Surf Proc Landforms 22:239-248

Brown RW, Gallagher K, Duane M (1994a) A quantitative assessment of the effects of magmatism on the thermal history of the Karoo sedimentary sequence. J Afr Ear Sci 18:227-243

Brown RW, Summerfield MA, Gleadow AJW (1994b) Apatite fission track analysis: Its potential for the estimation of denudation rates and implications for models of long term landscape development. *In:* Process Models and Theoretical Geomorphology. Kirkby MJ (ed), John Wiley and Sons Ltd, Chichester, p 23-53

Brown RW, Summerfield MA, Gleadow AJW (2002) Denudational history along a transect across the Drakensberg Escarpment of southern Africa derived from apatite fission track thermochronology. J Geophys Res 107: doi:10.1029/2001JB000745

Brown RW, Gallagher K, Gleadow AJW, Summerfield MA (2000) Morphotectonic evolution of the South Atlantic margins of Africa and South America. *In:* Geomorphology and Global Tectonics. Summerfield MA (ed) John Wiley and Sons Ltd, Chichester, p 257-283

Brown RW, Gallagher K, Johnson K, Cockburn HAP, Summerfield M.A, Gleadow AJW (2001) All landscapes, great and small: problems and strategies for deriving regional denudation histories from sparse data. Earth System Processes, Abst Geol Soc Amer and Geol Soc Lond, Edinburgh, Scotland, p 81

Brown RW, Rust DJ, Summerfield MA, Gleadow AJW, De Wit MCJ (1990) An accelerated phase of denudation on the south-western margin of Africa: evidence from apatite fission track analysis and the offshore sedimentary record. Nucl Tracks Rad Meas 17:339-350

Buck WR, Martinez F, Steckler MS, Cochran JR (1988) Thermal consequences of lithospheric extension: pure and simple. Tectonics 7:213-234

Burtner RL, Nigrini A, Donelick RA (1994) Thermochronology of Lower Cretaceous source rocks in the Idaho-Wyoming Thrust Belt. Bull Am Assoc Petrol Geol 78:1613-1636

Cande SC, Kent DV (1995) A new geomagnetic polarity time scale for the Late Cretaceous and Cenozoic. J Geophy Res 97:13917-13951

Cande SC, Mutter JC (1982) A revised identification of the oldest sea-floor spreading anomalies between Australia and Antarctica. Earth Planet Sci Lett 58:151-160

Carlson WD, Donelick RA, Ketcham RA (1999) Variability of apatite fission-track annealing kinetics: I. Experimental results. Am Mineral 84:1213-1223

Cercone KR (1984) Thermal history of Michigan Basin. Am Assoc Petrol Geol Bull 68:130−136

Cercone KR, Pollack HN (1991) Thermal maturity of the Michigan Basin. Geol Soc Am Spec Paper 256: 1-11

Collins WJ (1991) A reassessment of the 'Hunter-Bowen Orogeny': Tectonic implications for the southern New England Fold Belt. Aust J Earth Sci 38:409-423

Coney PJ, Edwards A, Hine R, Morrison F, Windrim D (1990) The regional tectonics of the Tasman orogenic system, eastern Australia. J Struct Geol 12: 519-543

Conrad CP, Gurnis M (2003) Seismic tomography, surface uplift, and the breakup of Gondwanaland: Integrating mantle convection backwards in time. Geochem Geophys Geosyst 4:1031, doi:10.1029/2001GC000299

Corfu F, Stone D (1998) The significance of titanite and apatite U-Pb ages: Constraints for the post-magmatic thermal-hydrothermal evolution of a batholitic complex, Berens River area, northwestern Superior Province, Canada. Geochim Cosmochim Acta 62:2979-2995

Corrigan J (1991) Inversion of apatite fission track data for thermal history information. J Geophys Res 96: 10374-10360

Coward MP, Daly MC (1984) Crustal lineaments and shear zones in Africa: their relationship to plate movements. Precamb Res 24:27-45

Coward MP, Potgieter R. (1983) Thrust zones and shear zones of the margin of the Namaqua and Kheis mobile belts, Southern Africa. Precamb Res 24:27-45

Crowley KD (1991) Thermal history of Michigan Basin and Southern Canadian Shield from apatite fission track analysis. J Geophys Res 96:697-711

Crowley KD (1993) Lenmodel – a forward model for calculating length distributions and fission-track ages in apatite. Computer Geosci 19:619-626

Crowley KD, Cameron M, Schaffer LR (1991) Experimental studies of annealing of etched fission tracks in fluorapatite. Geochim Cosmochim Acta 55:1449-1465

Daly MC, Chorowicz J, Fairhead JD (1989) Rift basin evolution in Africa: The influence of reactivated steep basement shear zones. *In:* Inversion Tectonics. Cooper MA, Williams GC (eds) Geol Soc Lond Spec Pub 44, p 309-334

Dingle RV, Siesser WG, Newton AR (1983) Mesozoic and Tertiary geology of southern Africa. AA Balkema, Rotterdam

Donelick RA (1993) Apatite etching characteristics versus chemical composition. Nucl Tracks Radiat Meas 21:604

Donelick RA, Ketcham RA, Carlson WD (1999) Variability of apatite fission-track annealing kinetics: II. Crystallographic orientation effects. Am Mineral 84:1224-1234

Donelick RA, O'Sullivan PB, Ketcham RA (2005) Apatite fission-track analysis. Rev Mineral Geochem 58: 49-94

Donelick RA, Roden MK, Mooers JD, Carpenter BS, Miller DS (1990) Etchable length reduction of induced fission tracks in apatite at room temperature (~23°C): crystallographic orientation effects and "initial" mean lengths. Nucl Tracks Radiat Meas 17:261-265

Duddy IR, Green PF, Bray RJ, Hegarty KA (1994) Recognition of the thermal effects of fluid flow in sedimentary basins. *In*: Geofluids; Origin. Migration and Evolution of Fluids in Sedimentary Basins. Parnell J (ed) Geol Soc Lond Spec Pub 78, p 325-345

Dumitru TA, Hill KC, Coyle DA, Duddy IR, Foster DA, Gleadow AJW, Green PF, Laslett GM, Kohn BP, O'Sullivan AB (1991) Fission track thermochronology: Application to continental rifting of southeastern Australia. Aust Petrol Exploration Assoc J 31:131-142

Eby GN, Roden-Tice M, Krueger HL, Ewing W, Faxon EH, Woolley AR (1995) Geochronology and cooling history of the northern part of the Chilwa Alkaline Province, Malawi. J Afr Earth Sci 20:275-288

Efron B, Tibshirani RJ (1993) An Introduction to the Bootstrap. Chapman and Hall, New York

Ehlers TA (2005) Crustal thermal processes and the interpretation of thermochronometer data. Rev Mineral Geochem 58:315-350

Ehlers TA, Farley KA (2003) Apatite (U-Th)/He thermochronometry: methods and applications to problems in tectonics and surface processes. Earth Planet Sci Lett 206:1-14

Erlank AJ, Marsh JS, Duncan AR, Miller RmcG, Hawkesworth CJ, Betton PJ, Rex DC (1984) Geochemistry and petrogenesis of the Etendaka volcanic rocks from SWA/Namibia. Spec Pub Geol Soc S Afr 13:195-245

Fairhead JD (1988) Mesozoic plate tectonic reconstructions of the Central-South Atlantic Ocean: the role of the west and central African Rift System. Tectonophys 155:181-191

Fairhead JD, Binks RM (1991) Differential opening of the Central and South Atlantic Ocean and the opening of the west African Rift System. Tectonophys 187:191-203

Farley KA (2002) (U-Th)/He dating: techniques, calibrations and applications. Rev Mineral Geochem 47: 819-843

Fergusson CL, Coney PJ (1992) Convergence and intraplate deformation in the Lachlan Fold Belt of southeastern Australia. Tectonophysics 214:417-439

Fischer JH, Barratt MW, Droste JB, Shaver R (1988). Michigan Basin. *In:* Sedimentary Cover - North American Craton: US. The Geology of North America vol D-2. Sloss LL (ed) Geol Soc Amer, Boulder, p 361-382

Foster DA, Gleadow AJW (1992a) The morphotectonic evolution of rift-margin mountains in central Kenya: Constraints from apatite fission track analysis. Earth Planet Sci Lett 113:157-171

Foster DA, Gleadow AJW (1992b) Reactivated tectonic boundaries and implications for the reconstruction of southeastern Australia and northern Victoria Land, Antarctica. Geology 20:267-270

Foster DA, Gleadow AJW (1993a) Episodic denudation in East Africa: A legacy of intracontinental tectonism. Geophys Res Lett 20:2395-2398

Foster DA, Gleadow AJW (1993b) The architecture of Gondwana rifting in southeastern Australia: evidence from apatite fission track thermochronology. *In:* Gondwana 8 - Assembly, Evolution and Dispersal. Findlay R, Unrug R, Banks RH, Veevers, JJ (eds) Balkema, Rotterdam, p 597-603

Foster DA, Gleadow AJW (1996) Structural framework and denudation history of the flanks of the Kenya and Anza Rifts. East Africa. Tectonics 15:258-271

Foster DA, Gray DR (2000) Evolution and structure of the Lachlan Fold Belt (Orogen) of Eastern Australia. Ann Rev Earth Planet Sci 28:47-80

Frisch W, Pohl W (1986) Petrochemistry of some mafic and ultramafic rocks from the Mozambique Belt, SE Kenya. Mitt Österr Geol Ges 78:97-114

Gallagher K (1995) Evolving temperature histories from apatite fission-track data. Earth Planet Sci Lett 136: 421-435

Gallagher K, Brown RW (1999a) Denudation and uplift at passive margins: the record on the Atlantic Margin of southern Africa. Phil Trans Roy Soc London A 357:835-859

Gallagher K, Brown RW (1999b) The Mesozoic denudation history of the Atlantic margins of southern Africa and southeast Brazil and the relationship to offshore sedimentation. *In:* The Oil and Gas Habitats of the South Atlantic. Cameron N, Bate R, Clure V (eds) Geol Soc London Special Pub 153, p 41-53

Gallagher K, Sambridge M (1994) Genetic algorithms: a powerful method for large scale non-linear optimisation problems. Computer Geosci 20:1229-1236

Gallagher K, Brown RW, Johnson C (1998) Fission track analysis and its applications to geological problems. Ann Rev Earth Planet Sci 26:519-572

Gallagher K, Dumitru TA, Gleadow AJW (1994a) Constraints on the vertical motion of eastern Australia during the Mesozoic. Basin Res 6:77-94

Gallagher K, Hawkesworth CJ, Mantovani MJ (1994b) The denudation history of the onshore continental margin of SE Brazil inferred from apatite fission track data. J Geophys Res 99:18,117-18,145

Gallagher K, Stephenson J, Brown R, Holmes C, Ballester P (2005) Exploiting 3D spatial sampling in inverse modeling of thermochronological data. Rev Mineral Geochem 58:375-387

Gilchrist AR, Summerfield MA (1994) Tectonic models of passive margin evolution and their implications for theories of long-term landscape development. *In:* Process Models and Theoretical Geomorphology. Kirkby MJ (ed) John Wiley and Sons, Chichester, p 55-84

Gleadow AJW (1980) Fission track age of the KBSTuff and associated hominid remains in northern Kenya. Nature 284:225-230

Gleadow AJW, Brown RW (2000) Fission track thermochronology and the long-term denudational response to tectonics. *In:* Geomorphology and Global Tectonics. Summerfield MA (ed) John Wiley and Sons Ltd, Chichester, p 57-75

Gleadow AJW, Duddy IR (1981) Early Cretaceous volcanism and early breakup history of southeastern Australia: Evidence from fission track dating of volcaniclastic sediments. *In:* Gondwana Five - Proceedings of the Fifth International Gondwana Symposium. Cresswell MM, Vella P (eds) Balkema, Rotterdam, p 295-300

Gleadow AJW, Lovering JF (1978a) Fission track geochronology of King Island, Bass Strait, Australia; relationship to continental rifting. Earth Planet Sci Lett 37: 429-437

Gleadow AJW, Lovering JF (1978b) Thermal history of granitic rocks from western Victoria : a fission track dating study. J Geol Soc Australia 25:323-340

Gleadow AJW, Belton DX, Kohn BP, Brown RW (2002a) Fission track dating of phosphate minerals and the thermochronology of apatite. Rev Mineral Geochem 48:579-630

Gleadow AJW, Duddy IR, Green PF, Lovering JF (1986) Confined fission track lengths in apatite: a diagnostic tool for thermal history analysis. Contrib Mineral Petrol 94:405-415

Gleadow A, Kohn B, Gallagher K, Cox S (1996) Imaging the thermotectonic evolution of eastern Australia during the Mesozoic from fission track dating of apatites. *In:* Mesozoic Geology of the Eastern Australia Plate Conference, Geol Soc Aust Abstr 43, p 195-204

Gleadow AJW, Kohn BP, Brown RW, O'Sullivan PB, Raza, A (2002b) Fission track thermotectonic imaging of the Australian continent. Tectonophysics 349:5-21

Gray DR (1997) Tectonics of the southeastern Australian Lachlan Fold Belt: structural and thermal aspects. *In:* Orogeny Through Time. Burg JP, Ford M (eds) Geol Soc Lond Spec Pub 121, p 149-177

Green PF (1988) The relationship between track shortening and fission track reduction in apatite: combined influences of inherent instability, annealing anisotropy, length bias and system calibration. Earth Sci Planet Lett 89:335-352

Green PF, Duddy IR, Gleadow AJW, Tingate PR, Laslett GM (1985) Fission track annealing in apatite: Track length measurements and the forms of the Arrhenius Plot. Nucl Tracks 10:323-328

Green PF, Duddy IR, Laslett GM, Hegarty KA, Gleadow AJW, Lovering JF (1989) Thermal annealing of fission tracks in apatite, 4. Quantitative modeling techniques and extension to geological timescales. Chem Geol 79:155-182

Greene LC, Richards DR, Johnson RA (1991) Crustal structure and tectonic evolution of the Anza Rift, Northern Kenya. Tectonophys 197:203-211

Gregory JW (1896) The Great Rift Valley. London, John Murray

Guillou-Frottier L, Mareschal JC, Jaupart C, Gariepy C, Lapointe R, Bienfait G (1995) Heat flow variations in the Grenville Province, Canada. Earth Planet Sci Lett 136:447-460

Gunnell Y, Gallagher K, Carter A, Widdowson M, Hurford AJ (2003) Denudation history of the continental margin of western penisular India since the early Mesozoic – reconciling apatite fission-track data with geomorphology. Earth Sci Planet Lett 6761:1-15

Gurnis M, Mitrovica JX, Ritsema J, van Heijst H-J (2000) Constraining mantle density structure using geological evidence of past uplift rates: the case of the African Superplume. Geochem Geophys Geosyst 1, doi:10.1029/1999GC000035

Harrington HJ, Korsch RJ (1985) Tectonics of the New England Orogen. Aust J Earth Sci 32:163-179

Harrison TM, Grove M, Lovera O (2005) Time-temperature paths from K-feldspar $^{40}Ar/^{39}Ar$ and monazite U/Pb dating. *In:* Thermochronology. Reiners PW, Ehlers TA (eds), Rev Min Geochem XX:xxx-xxx

Hasebe N, Barbarand J, Jarvis K, Carter A, Hurford AJ (2004) Apatite fission track chronometry using laser ablation-ICP-MS. Chem Geol 207:135-145

Hawkesworth CJ, Gallagher K, Kelley S, Mantovani M, Peate D.W, Regelous M, Rogers N (1992) Paraná magmatism and the opening of the South Atlantic. *In* Magmatism and the Causes of Continental Break-Up. Storey BC, Alabaster T, Pankhurst RJ (eds) Geol Soc Spec Pub 68, p 221-240

Hill KC, Hill KA, Cooper GT, O'Sullivan AJ, O'Sullivan PB, Richardson J (1995) Inversion around the Bass Basin, SE Australia. *In:* Basin Inversion. Buchanan JG, Buchanan PG (eds) Geol Soc Lond Spec Pub 88, p 525-547

Hoffman PF (1988) United Plates of America, the birth of a craton: Early Proterozoic assembly and growth of Laurentia. Ann Rev Earth Planet Sci 16:543-603

House MA, Wernicke BP, Farley KA (1998) Dating topography of the Sierra Nevada, California, using apatite (U-Th)/He ages. Nature 396:66-69

Isaaks EH, Srivastava RM (1989) Introduction to Applied Geostatistics, Oxford University Press

Issler DR (1996) Optimising time-step size for apatite fission-track annealing models. Computer Geosci 22: 67-74

Johnson BD, Veevers JJ (1984) Oceanic paleomagnetism. *In:* Phanerozoic History of Australia. Veevers JJ (ed) Clarendon Press, Oxford, p 17-38

Ketcham RA (2005) Forward and inverse modeling of low-temperature thermochronometry data. Rev Mineral Geochem 58:275-314
Ketcham RA, Donelick RA, Carlson WD (1999) Variability of apatite fission-track annealing kinetics: III. Extrapolation to geological time scales. Am Mineral 84:1235-1255
Ketcham RA, Donelick RA, Donelick MB (2000) AFTSolve: A program for multi-kinetic modeling of apatite fission-track data. Geol Mater Res 2
Kohn BP, Gleadow AJW, Cox, SJ (1999) Denudation history of the Snowy Mountains: constraints from apatite fission track thermochronology Aust J Earth Sci 46:181- 198
Kohn BP, Gleadow, AJW, Brown RW, Gallagher K, O'Sullivan PB, Foster DA (2002) Shaping the Australian crust over the last 300 million years: Insights from fission track thermotectonic and denudation studies of key terranes. Aust J Earth Sci 49:697-717
Kohn BP, O'Sullivan PB, Gleadow AJW, Brown RW, Gallagher K, Foster DA (2003) Fission track thermotectonic imaging and denudation history of Tasmania: Reply to Discussion by D.E. Leaman. Aust J Earth Sci 50:646-650
Kooi H, Beaumont C (1994) Escarpment evolution on high-elevation rifted margins: Insights derived from a surface processes model that combines diffusion, advection and reaction. J Geophys Res 99:12191-12209
Kreuser T, Wopfner H, Kaaya CZ, Markwort S, Semkiwa PM, Aslanidis P (1990) Depositional evolution of Permo-Triassic Karoo basins in Tanzania with reference to their economic potential. J Afr Earth Sci 10: 151-167
Kumarapelli PS (1985) Vestiges of Iapetan rifting in the craton west of the Northern Appalachians. Geosci Canada 12:54-59
Lambiase JJ (1989) The framework of African rifting during the Phanerozoic. J Afr Earth Sci 8:183-190
Laslett GM, Galbraith RF (1996) Statistical modeling of thermal annealing of fission tracks in apatite. Geochim Cosmochim Acta 60:5117-5131
Laslett GM, Green PF, Duddy IR, Gleadow AJW (1987) Thermal annealing of fission tracks in apatite, 2. A quantitative analysis. Chem Geol 65:1-13
Lister GS, Etheridge MA (1989) Detachment model for the uplift and volcanism of the Eastern Highlands. *In:* Intraplate Volcanism in Eastern Australia and New Zealand. Johnson W (ed) Cambridge Univ Press, New York, p 297-312
Lithgow-Bertelloni C, Silver PG (1998) Dynamic topography, plate driving forces and the African superswell. Nature 395:296-272
Lorencak M (2003) Low temperature thermochronology of the Canadian and Fennoscandian Shields: Integration of apatite fission track and (U-Th)/He methods. PhD thesis University of Melbourne
Lorencak M, Kohn BP, Osadetz KG, Gleadow AJW (2004) Combined apatite fission track and (U-Th)/He thermochronometry in a slowly cooled terrane: Results from a 3440 m deep drill hole in the southern Canadian Shield. Earth Planet Sci Lett 227:87-104
Lucas SB, St-Onge MR (eds) (1998) Geology of the Precambrian Superior and Grenville Provinces and Precambrian fossils in North America. Geol Canada No 7, Geol Surv Canada (also Geol Soc Amer, The Geology of North America, Decade Nth Amer Proj Vol C1)
Lutz TM, Omar GI (1991) An inverse method of modeling thermal histories from apatite fission-track data. Earth Planet Sci Lett 104:181-195
Mareschal JC, Jaupart C, Gariepy C, Cheng LZ, Guillou-Frottier L, Bienfait G, Lapointe R (2000) Heat flow and deep thermal structure near the southeastern edge of the Canadian Shield. Can J Earth Sci 37:399-414
Martin H (1953) Notes on the Dwyka succession and on some pre-Dwyka valleys in South West Africa. Trans Geol Soc S Afr 56:37-43
Martin H (1973) The Atlantic margin of southern Africa between latitude 17° south and The Cape of Good Hope. *In:* The Ocean Basins and Margins Vol 1, The South Atlantic. Nairn AEM, Stehli F (eds) Plenum Press, NY, p 277-300
Mayne SJ, Nicholas E, Bigg-Wither AL, Rasidi JS, Raine MJ (1974) Geology of the Sydney Basin – A Review. Bur Min Res Aust Bull 149
Mbede EI, Hurford A, Ebinger CJ, Schandelmeier H (1993) A constraint on the uplift history of the Rukwa Rift, SW. Tanzania: A reconnaissance apatite fission track analysis. Mus Roy Afr Cent Tervuren (Belg), Dept Geol Min Rapp Ann 1991-1992:99-108
McDougall I, Harrison TM (1999) Geochronology and Thermochronology by the $^{40}Ar/^{39}Ar$ Method. Oxford Monographs on Geology and Geophysics 9 (2nd Ed) Oxford University Press, New York
Miller JMcL, Phillips D, Wilson CJL, Dugdale LD (2004) A new tectonic model for the Delamerian and western Lachlan Orogens. Geol Soc. Austral Abst 73: p 174
Mitas L, Mitasova H (1995) Interpolation by regularized spline with tension: 1. theory and implementation. Math Geol 25:641-655

Möller A (1995) Pan- African granulites and Early Proterozoic eclogites in the Precambrian basement of eastern Tanzania: P-T-t history and crustal evolution of the complex Mozambique Belt. PhD thesis, Kiel Univ

Moore ME, Gleadow AJW, Lovering JF (1986) Thermal evolution of rifted continental margins: new evidence from fission track dating of apatites from southeastern Australia. Earth Planet Sci Lett 78:255-270

Morley CK, Wescott WA, Stone DM, Harper RM, Wigger ST, Karanja FM (1992) Tectonic evolution of the northern Kenyan Rift. J Geol Soc Lond 149:333-34

Muhongo S (1989) Tectonic setting of the Proterozoic metamorphic terrains in eastern Tanzania and their bearing on the evolution of the Mozambique Belt. IGCP No. 255 Newslett Bull 2:43-50

Munyanyiwa H (1993) Thermobarometry of mafic rocks within the Zambezi Mobile Belt, northern Zimbabwe. *In:* Proc Eighth Gondwana Symp. Finlay RH, Unrug R, Banks MR, Veevers JJ (eds) Balkema, Rotterdam, p 83-95

Noble PW (1997) Post Pan African tectonic evolution of Eastern Africa: an apatite fission track study. PhD thesis, La Trobe University

Noble WP, Foster DA, Gleadow AJW (1997) The post Pan African tectonothermal development of the Mozambique belt in Eastern Tanzania. Tectonophys 275:331-350

Norvick MS, Smith MA (2001) Mapping the plate tectonic reconstruction of southern and southeastern Australia and implications for petroleum systems. APPEA J 41:15-35

Nunn JA, Sleep NH, Moore WE (1984) Thermal subsidence and generation of hydrocarbons in Michigan Basin. Am Assoc Petrol Geol Bull 68:296-315

Nürnburg D, Müller RD (1991) The tectonic evolution of the South Atlantic from late Jurassic to present. Tectonophys 191:27-53

O'Sullivan PB, Kohn BP (1997) Apatite fission track thermochronology of Tasmania. Aust Geol Surv Org Record 1997/35

O'Sullivan PB, Belton DX, Orr M (2000a) Post-orogenic thermotectonic history of the Mount Buffalo region, Lachlan fold belt, Australia; evidence for Mesozoic to Cenozoic. Tectonophysics. 317:1-26

O'Sullivan PB, Kohn BP, Cranfield L (1999b) Fission track constraints on the Mesozoic to Recent thermotectonic history of the northern New England Orogen, southeastern Queensland. *In*: New England Orogen, Proceedings of the NEO Conference. Flood PG (ed) University of New England Press, Armidale, p 285-293

O'Sullivan PB, Coyle DA, Gleadow AJW, Kohn BP (1996b) Late Mesozoic to Early Cenozoic thermotectonic history of the Sydney Basin and the eastern Lachlan Fold Belt, Australia. *In* Mesozoic Geology of the Eastern Australia Plate Conference, Geol Soc Aust Abst 43, p. 424-432

O'Sullivan PB, Foster DA, Kohn BP, Gleadow AJW (1996a) Multiple post orogenic denudation events: An example from the eastern Lachlan fold belt, Australia. Geology 24:563-566

O'Sullivan PB, Kohn BP, Foster DA, Gleadow AJW (1995b) Fission track data from the Bathurst batholith: Evidence for rapid mid-Cretaceous uplift and erosion within the eastern highlands of Australia. Aust J Earth Sci 42:597-607

O'Sullivan PB, Orr M, O'Sullivan AJ, Gleadow AJW (1999a) Episodic Late Paleozoic to Recent denudation of the Eastern Highlands of Australia: evidence from the Bogong High Plains, Victoria. Austral J Earth Sci 46:199-216

O'Sullivan PB, Foster DA, Kohn BP, Gleadow AJW, Raza A (1995a) Constraints on the dynamics of rifting and denudation on the eastern margin of Australia: Fission track evidence for two discrete causes of rock cooling. Aust Inst Min Metal Publ 9/95:441-446

O'Sullivan PB, Gibson DL, Kohn BP, Pillans B, Pain CF (2000b) Long-term landscape evolution of the Northparkes region of the Lachlan Fold Belt, Australia: Constraints from fission track and omagnetic data. J Geol 108:1-16

O'Sullivan PB, Mitchell MM, O'Sullivan AJ, Kohn BP, Gleadow AJW (2000c) Thermotectonic history of the Bassian Rise, Australia: Implications for the breakup of eastern Gondwana along Australia's southeastern margins. Earth Planet Sci Lett 182:31-47

Patchett PJ, Embry AF, Ross GM, Beauchamp B, Harrison JC, Mayr U, Isachsen CE, Rosenberg EJ, Spence GO (2004) Sedimentary cover of the Canadian Shield through Mesozoic time reflected by Nd isotopic and geochemical results for the Sverdrup Basin, Arctic Canada. J Geol 112:39-57

Palfreyman WD (1984) Guide to the Geology of Australia. Bur Min Res Bull 181:111p.

Partridge TC (1993) The evidence for Cainozoic aridification in southern Africa. Quat Int 17:105-110

Pollack HN, Hurter S J, Johnson JR (1993) Heat flow from the Earth's interior: Analysis of the global data set. Rev Geophys 31:267-280

Raab MJ, Brown RW, Gallagher K, Carter A, Weber K (2002) Late Cretaceous reactivation of major crustal shear zones in northern Namibia: constraints from apatite fission track analysis. Tectonophys 349:75-92

Rach NM, Rosendahl BR (1989) Tectonic controls of the Speke Gulf. J Afr Ear Sci 8:471-488

Reeves CV, Karanja FM, MacLeod IN (1987) Geophysical evidence for a failed Jurassic rift and triple junction in Kenya. Earth Planet Sci Lett 81:299-311
Reiners PW (2005) Zircon (U-Th)/He thermochronometry. Rev Mineral Geochem 58:151-179
Reiners PW, Farley KA (1999) Helium diffusion and (U-Th)/He thermochronometry of titanite. Geochim Cosmochim Acta 63:3845-3859
Renne PR, Glen JM, Milner SC, Duncan AR (1996) Age of Etendeka flood volcanism and associated intrusions in southwestern Africa. Geology 24:659-662
Rosendahl BR (1987) Architecture of continental rifts with special reference to East Africa. Ann Rev Earth Planet Sci 15:445-503
Rust DJ Summerfield MA (1990) Isopach and borehole data as indicators of rifted margin evolution in southwestern Africa. Mar Pet Geol 7:277-287
Sambridge M, Braun J, McQueen H (1995) Geophysical parameterization and interpolation of irregular data using natural neighbor. Geophys J Int 122:837-857
Sanford BV, Thompson FJ, McFall GH (1985) Plate tectonics - a possible controlling mechanism in the development of hydrocarbon traps in southwest Ontario. Bull Canad Petrol Geologists 33:52-71
Sass JH, Lachenbruch AH (1979) The thermal regime of the Australian continental crust. *In*: The Earth – Its Origin, Structure and Evolution. McElhinny MW (ed) Academic Press, New York, p 301-352
Shackleton RM (1986) Precambrian collision tectonics in Africa. *In*: Collision Tectonics. Coward MP, Ries AC (eds) Geol Soc Lond Spec Pub 19, p 329-349
Smith M (1994) Stratigraphic and structural constraints on mechanisms of active rifting in the Gregory rift, Kenya. Tectonophys 236:1-2
Smith M, Mosley P (1993) Crustal heterogeneity and basement influence on the development of the Kenya rift, East Africa. Tectonics 12:591-606
Smith WHF, Wessel P (1990) Gridding with continuous splines in tension, Geophysics 55:293-305
Söhnge APG, Hälbich IW (1983) Geodynamics of the Cape Fold Belt. Geol Soc S Afr Spec Pub 12
Stagman JG (1978) An Outline of the Geology of Rhodesia. Rhodesia Geol Surv Bull 80
Steckler MS, Omar GI, Karner GD, Kohn BP (1993) Pattern of hydrothermal circulation within the Newark Basin from fission-track analysis. Geology 21:735-738
Stern RJ (1994) Arc assembly and continental collision in the Neoproterozoic East African Orogeny. Ann Rev Earth Plan Sci 22:319-351
Tagami T (2005) Zircon fission-track thermochronology and applications to fault studies. Rev Mineral Geochem 58:95-122
Tagami T, O'Sullivan PB (2005) Fundamentals of fission-track thermochronology. Rev Mineral Geochem 58: 19-47
Tankard AJ, Jackson MP, Eriksson KA, Hobday DK, Hunter DR, Minter WEL (1982) Crustal Evolution of Southern Africa: 3.8 Billion Years of Earth History, Springer-Verlag, New York
Thomas DSG Shaw PA (1990) The deposition and development of the Kalahari Group sediments, Central Southern Africa, J Afr Earth Sci 10:187-197
Thurston PC, Williams HR, Sutcliffe RH, Stott GM (eds) (1991) Geology of Ontario. Ontario Geol Surv Spec Vol 4, Parts I and II
Unternehr P, Curie D, Olivet JL, Goslin J, Beuzart P (1988) South Atlantic fits and intraplate boundaries in Africa and South America. Tectonophysics 155:169-179
Van den haute P (1984) Fission track ages of apatites from the Precambrian of Rwanda and Burundi: relationship to East African rift tectonics. Earth Planet Sci Lett 71:129-140
van der Beek P (1995) Tectonic evolution of rifts: inferences from numerical modeling and fission track thermochronology. PhD thesis Vrije Universiteit
van der Beek P, Mbede E, Andriessen PAM, Delvaux, D (1998) Denudation of the Malawi and Rukwa rift flanks (East African System) from apatite fission track thermochronology. J Afr Earth Sci 26:363-385
van der Beek PA, Braun J, Lambeck K (1999) Post-Paleozoic uplift history of southeastern Australia revisited: results from a process-based model of landscape evolution. Aust J Earth Sci 46:157-172
Veevers JJ (ed) (1984) Phanerozoic Earth History of Australia. Clarendon Press Oxford
Veevers JJ, Powell C McA, Roots SR (1991) Review of seafloor spreading around Australia. I. Synthesis of the patterns of spreading. Aust J Earth Sci 38:373-389
Veevers JJ (2000) Changes of tectono-stratigraphic regime in the Australian plate during the 99 Ma (mid-Cretaceous) and 43 Ma (mid-Eocene) swerves of the Pacific. Geology 28:47-50
Visser JNJ (1987) The paleogeography of part of southwestern Gondwana during the Permo-Carboniferous glaciation. Paleogeog Paleoclim Paleoecol 61:205-219
Visser JN (1995) Post-glacial Permian stratigraphy and geography of southern and central Africa: boundary conditions for climatic modeling. Paleogeog Paleoclim Paleoecol 118:213-243

Viviers MC, de Azevedo RLM (1988) The southeastern area of the Brazilian continental margin: its evolution during the middle and late Cretaceous as indicated by paleoecological data. Revista Bras Geosci 18: 291-298

Wagner GA, Van den haute P (1992) Fission–Track Dating. Enke Verlag – Kluwer Academic Publishers, Dordrecht

Wagner M, Altherr R, Van den haute P (1992) Apatite fission-track analysis of Kenyan basement rocks: Constraints on the thermotectonic evolution of the Kenya dome. A reconnaissance study. Tectonophys 204:93-110

Ward JD (1988) Geology of the Tsondab Sandstone Formation. J Sed Geol 55:143-162

Waschbusch P, Beaumont C, Korsch RJ (1999) Geodynamic modeling of aspects of the New England Orogen and adjacent Bowen, Gunnedah and Surat basins. *In:* New England Orogen. Proceedings of the NEO Conference. Flood PG (ed) University of New England Press, Armidale, p. 204-210

Weber UD, Hill KC, Brown RW, Gallagher K, Kohn BP, Gleadow AJW, Foster DA (2004) Sediment supply to the Gippsland Basin from thermal history analysis: constraints on Emperor-Golden Beach reservoir composition. APPEA J 44:397-415

Weissel JK, Hayes DE (1977) Evolution of the Tasman Sea re-appraised. Earth Planet Sci Lett 36:77-84

Wessel P, Smith WHF (1991) Free software helps map and display data, EOS Trans Am Geophys Union 72: 445-446

Willett SD (1997) Inverse modeling of annealing of fission tracks in apatite 1: A Controlled random search method. Am J Sci 297:939-969

Winn RD, Steinmetz JC, Kerekgyarto WL (1993) Stratigraphy and rifting history of the Mesozoic-Cenozoic Anza Rift, Kenya. Am Assoc Petrol Geol Bull 77:1989-2005

Wopfner H (1986) Evidence for Late Paleozoic glaciation in southern Tanzania. Palaegeog Paleoclim Paleoecol 56:259-275

Wopfner H, Kaaya CZ (1991) Stratigraphy and morphotectonics of Karoo deposits of the Northern Selous Basin, Tanzania. Geol Mag 128:319-334